Basin-wide particulate carbon flux in the Atlantic Ocean: regional export patterns and potential for atmospheric CO_2 sequestration

Avan N. Antia, Wolfgang Koeve,[1]
Institut für Meereskunde, Kiel, Germany
Gerd Fischer,
Fachbereich Geowissenschaften, Universität Bremen, Bremen, Germany
Thomas Blanz,[2] Detlef Schulz-Bull,[2]
Institut für Meereskunde, Kiel, Germany
Jan Scholten,
Geologisches Institut, Universität Kiel, Kiel, Germany.
Susanne Neuer,
Arizona State University, Department of Biology, U.S.A.
Klaus Kremling, Joachim Kuss,[2] Rolf Peinert,
Institut für Meereskunde, Kiel, Germany
Dirk Hebbeln,
Fachbereich Geowissenschaften, Universität Bremen, Bremen, Germany
Uli Bathmann,
Alfred Wegener Institut für Polarforschung, Bremerhaven, Germany
Maureen Conte
Woods Hole Ocenaographic Institution, Woods Hole, U.S.A.
Uwe Fehner, B. Zeitzschel
Institut für Meereskunde, Kiel, Germany

Corresponding author: A.N. Antia: aantia@ifm.uni-kiel.de

"Running head": ANTIA ET AL.: ATLANTIC OCEAN CARBON FLUX

accepted to *Global Biogeochemical Cycles*

[1] A. N. Antia, W. Koeve, K. Kremling, R. Peinert, U. Fehner, B. Zeitzschel, Institut für Meereskunde, Forschungsbereich Biogeochemie, Düsternbrooker Weg 20, 24145 Kiel, Germany (aantia@ifm.uni-kiel.de, w.koeve@sciencenet.com, kkremling@ifm.uni-kiel.de, rpeinert@sfb313.uni-kiel.de)

T. Blanz, D. Schulz-Bull, J. Kuss, Insitut für Ostseeforschung-Warnemünde, Seestrasse 15, 18119 Warnemünde, Germany (thomas.blanz@io-warnemuende.de, detlef.schulz-bull@io-warnemuende.de)

G. Fischer, D. Hebbeln, Fachbereich Geowissenschaften, Universität Bremen, Klagenfurter Strasse, 28359 Bremen, Germany (g05f@zfn.uni-bremen.de, dhebbeln@uni-bremen.de)

J. Scholten, Geologisches Institut, Universität Kiel, 24118 Kiel, Germany (js@gpi.uni-kiel.de)

S. Neuer, Arizona State University, Department of Biology, Tempe, AZ 85287-1501, U.S.A. (susanne.neuer@asu.edu)

U. Bathmann, Alfred Wegener Institut für Polarforschung, Bremerhaven, Germany. (ubathmann@awi-bremerhaven.de)

M. Conte, Woods Hole Ocenaographic Institution, Woods Hole, MA 02540, U.S.A. (mconte@whoi.edu)

(Received xxxx, 2000; revised xxxx, 2001;
accepted xxxxx, 2001.)

[1] Also at Laboratoire d'Etudes en Geophysique et Oceanographie Spatiale, Toulouse, France.

[2] Now at Institut für Ostseeforschung-Warnemünde, Warnemünde, Germany.

Paper number xxxxxxxxxx

Abstract

Particle flux data from 27 sites in the Atlantic Ocean have been compiled with a view to determining regional variations in the strength and efficiency of the biological pump and quantifying basin-wide fluxes and estimating the potential oceanic sequestration of atmospheric CO_2. An algorithm is derived relating annual particulate organic carbon (POC) flux to primary production and depth that yields variations in the Export Ratio (ER = POC FLUX/Primary Production) at 125 m of between 0.1 and 0.4 over the range of production from 50 to 400 $gCm^{-2}yr^{-2}$. Significant regional differences in changes of the ER with depth are related to the temporal stability of flux. Sites with more pulsed export have higher shallow ERs and show more rapid degradation of particulate organic carbon (POC) flux with depth, resulting in little variation in fluxes below ca. 3000 m. The opposing effects of organic carbon production and calcification on ΔpCO_2 of surface seawater are combined to calculate an "effective carbon flux" at the depth of euphotic zone and at the base of the winter mixed layer. POC flux at the base of the euphotic zone between 65°N and 65°S amounts to 3.14 $GtCyr^{-1}$, of which 5.7% is remineralised above the winter mixed layer, and is thus not available to sequestration on climatically relevant time scales. The effective carbon flux, termed J_{eff}, amounts to 2.47 $GtCyr^{-1}$ and is a measure of the potential sequestration of atmospheric CO_2 for the area considered. A shift in the composition of sedimenting particles (opal: carbonate ratio) is seen across the entire North Atlantic, indicating a basin-wide phenomenon that may be related to large-scale changes in climatic forcing.

Keywords: ocean carbon flux, rain ratio, carbon sequestration, Atlantic Ocean, biological pump

1. Introduction

Publications dealing with carbon flux in the ocean often introduce the issue in terms of the biological pump, ostensibly drawing down (anthropogenic) CO_2 from the atmosphere, with the potential to shape and/or modulate climate. Although in the framework of climatic processes the physical pump dominates in strength, the biological pump (through particle formation and vertical export) is the only process driving gradients in seawater carbonate chemistry over physical boundaries. Globally, sinking particles transfer about 0.4 GtC from the ocean surface to deeper water masses (Lampitt and Antia, 1997; Schlitzer, 1999) and to the sediment surface (Jahnke, 1996). Perhaps more importantly, biology responds to changes in climatic conditions in a manner that is complex and can be non-linear, triggering shifts in functional groups of organisms that change the oceans` biogeochemical functioning (e.g. Karl et al., 1997; Riebesell et al., 2000).

A major goal of the Joint Global Ocean Flux Study (JGOFS) has been to better understand the physical and biological conditions that control regional variations in the strength and efficiency of the biological pump. The net effect of the biological pump on draw-down of atmospheric CO_2 depends on three main characteristics. Firstly, the mode and speed of particle sinking determines the depth to which particles are exported and the degree to

which they are remineralised in the water column. Empirical studies have yielded algorithms linking primary production to particulate organic carbon (POC) flux and water depth (e.g. Suess, 1980; Pace et al., 1987; Berger et al., 1987) that are useful to calculate the fraction of productivity that is exported (i.e. the Export Ratio, ER = POC Flux/Primary Production). There are significant regional differences in ER normalised to a single depth (e.g. ER_{2000m} by Lampitt and Antia, 1997; ER_{1000m} by Fischer et al., 2000). Yet little is known of regional and temporal variations in the degree of decrease of POC flux with depth, that results from differences in the mode of export and composition of sedimenting particles.

Secondly, the draw-down of atmospheric CO_2 is a function not just of the organic tissue pump but results from the ratio of organic (POC) to inorganic carbon (PIC=calcite+aragonite) in export, termed the rain ratio (RR=POC:PIC), since photosynthesis and calcification have

opposing effects on pCO_2 of the surface water that is in contact with the atmosphere (Frankignoulle et al., 1994; Archer and Meier-Reimer, 1994). The Rain Ratio is thus a measure of the "efficiency" of biological carbon sequestration. The carbonate (alkalinity) pump changes the totalC: totalN ratio of export and has an effect on ΔpCO_2 between the atmosphere and surface ocean that is decoupled from the ratio of carbon to the limiting nutrient in sub-thermocline upwelled water. Globally there are large variations in the rain ratio (POC:PIC) in sedimenting particles, with higher ratios in the Pacific than Atlantic Ocean, and higher rain ratios in polar regions and at continental margins than in the non-polar open ocean (Tsunogai and Noriki, 1991).

Thirdly, it is important to emphasise that for carbon export to be effective on climatically relevant time scales, particles must leave the seasonally mixed layer, i.e. that layer which is mixed at least once during winter overturning. The widely used concept of new production and export production (Dugdale and Goering, 1967; Eppley and Peterson, 1979) equates the sum of allochthonous nitrogen inputs into the euphotic zone through vertical mixing, nitrogen fixation and other external sources with the downward fluxes of particulate organic nitrogen (PON) and dissolved organic nitrogen (DON). Since DON fluxes at the base of the euphotic zone may not be negligible, particulate organic matter flux can approximate but probably never equal new production. Equating new production to export production and using global and regional estimates of new production (Falkowski et al., 1998; Oschlies and Garcon, 1998) thus allows calculation of the fraction of primary production available to export in organic particles. New Production does not, however, quantify carbon export in any climatically relevant sense since a) the CO_2 released during respiration (or taken up by during calcite dissolution) equilibrates with the atmosphere to the depth of maximal seasonal ventilation and not the euphotic depth and b) the net effect of biology on seawater pCO_2 must include calcite formation and export, that is decoupled from new production. Highest POC remineralisation (e.g. Suess, 1980) and calcite dissolution (Millimann, 1999) rates occur between the euphotic zone and the winter mixed layer (WML) depth; in this depth horizon export production and sequestration diverge.

Quantification and characterisation of the biological pump was a central goal of the Joint Global Ocean Flux (JGOFS) study, and a large amount of data is now available from long-term sediment traps deployed in the Atlantic Ocean. Though the use of sediment traps has its own caveats, it has the strength that it is based on actual measurements that reveal qualitative information that has greatly enhanced our understanding of biogeochemical cycling in the oceans. A major problem, as we show, is the uncertainty of the efficiency of traps in collecting sinking particles (Gust et al., 1994, Scholten et al., 2001).

In this paper we use a compilation of sediment trap data from 27 sites in the Atlantic Ocean to determine the role of the biological pump in transfer of carbon to the oceans' interior and its regional characteristics and variability. We estimate the basin-wide potential of the biological pump for carbon sequestration from the atmosphere and its dependence on local production. We also concentrate on determining regional variations in flux characteristics and export efficiency, since these are important to predicting the response of the biological pump to changes in climatic forcing.

2. Materials and Methods

Data base: Data have been collated from 27 sites (Figure 1, for site acronyms see also Table 1) where particle interceptor traps were deployed in the Atlantic Ocean between 80°N and 65°S. Traps were conical traps with an opening of approx. 0.5 m^2, deployed on bottom-anchored moorings for at least one year. Sample treatment varied in the addition of brine, use of fixative/poison, and methods of splitting and analytical procedure. Swimmers were removed from all samples either by manual picking under a binocular microscope or by passage through a sieve and subsequent rinsing. For details of mooring deployment and sample treatment the reader is referred to the original papers listed in Table 1.
Individual samples were integrated over 7 to 65 days, with longer intervals during periods of low, constant flux. Dry Weight, particulate organic carbon and nitrogen (POC, PON), carbonate, particulate biogenic silica and lithogenic material

were reported in mg $m^{-2}d^{-1}$. Inorganic carbon is calculated as 12% of calcium carbonate by weight and opal calculated from particulate biogenic silica using a molecular weight of 67.2 (Mortlock and Fröhlich, 1989). For the Sargasso Sea (OFP data) $CaCO_3$, POC/PON and opal (for part of the data set) were determined on the <0.125 mm fraction (both the 0.37 – 0.125 mm and <0.37 mm fractions were analysed separately and used to calculate the <0.125 mm fraction. Opal fluxes are not corrected for leaching in the trap samples, as this was not measured in all studies. Where lithogenic fluxes were not reported, these are calculated as a difference between total flux and its biogenic components (Lithogenic flux = mass flux – [carbonate + POC*2.2 + opal]). The loss of POC to the dissolved phase can potentially cause a large underestimation of flux in shallow traps (Noji et al., 1999; Kähler and Bauerfeind, 2001), but appears not to be significant in deeper traps (Kähler, pers. comm.). DOC was not determined for most traps in this study.

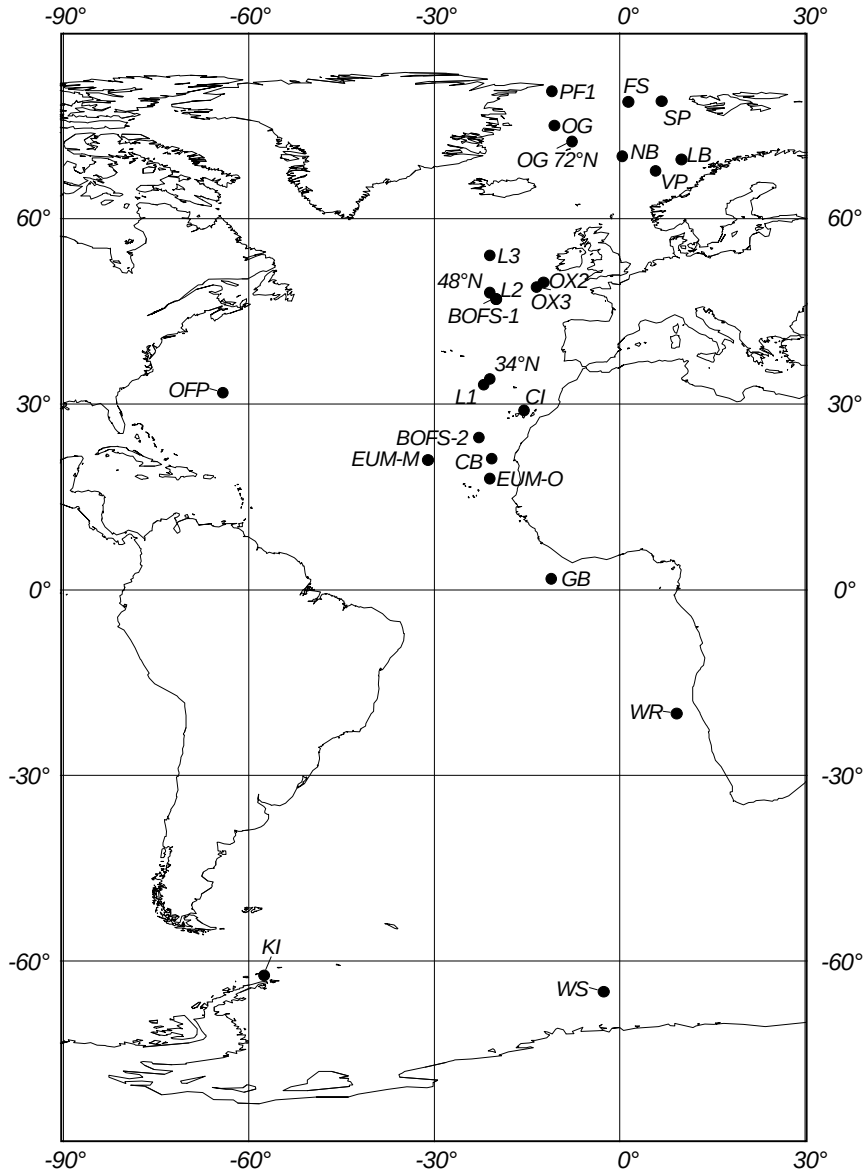

Figure 1: Locations of moorings from which data are used from this study. Station abbreviations are as listed in Table 1

.

Table 1: Mooring sites, bulk fluxes, trap collection efficiencies and data sources of data used in this study

Mooring Site	ID	Water Depth (m)	Trap Depth (m)	Lat. °N	Long. °W	Start [Date]	End [Date]	Interval (days)	Total Mass (g $m^{-2}yr^{-1}$)	POC	Trap Efficiency (%)[a]	Source
NE Polynya	PF1	295	130	80.5	11.0	02.08.92	02.08.93	365	11.19	1.10		Bauerfeind et al., 1997
NE Polynya		335	130	80.4	14.6	02.08.92	02.08.93	365	4.71	0.42		Bauerfeind et al., 1997
Spitzbergen	SP	1676	1125	78.9	-6.8	09.12.88	09.12.89	365	183.3	6.66		Hebbeln, 2000
Fram Strait	FS	2821	2440	78.8	-1.4	19.08.84	31.08.85	377	6.70	0.44		Honjo et al., 1988
Fram Strait		2487	1488	78.8	-0.2	01.07.87	15.06.88	350	60.40	3.06		Hebbeln & Wefer, 1991
Fram Strait		1763	1191	78.4	4.1	01.07.88	29.05.89	332	2.89	0.29		Hebbeln & Wefer, 1991
East Greenland Sea (75°N)	OG 75°N	3073	500	75.0	10.6	23.07.94	23.07.95	365	77.39	4.23		Peinert et al., 2000
East Greenland Sea (75°N)		3073	2000	74.6	10.4	10.08.94	11.10.95	427	66.54	2.18		Peinert et al., 2000
East Greenland Sea (72°N)	OG 72°N	2624	500	72.4	7.7	25.02.91	25.02.92	365	10.89	1.69		von Bodungen et al., 1995
East Greenland Sea (72°N)		2240	500	72.1	7.0	18.02.89	02.03.90	377	24.54	3.69		von Bodungen et al., 1995
East Greenland Sea (72°N)		2631	1000	72.4	7.7	25.02.91	25.02.92	365	11.20	1.17		von Bodungen et al., 1995
East Greenland Sea (72°N)		2631	2200	72.4	7.7	25.02.91	25.02.92	365	11.67	0.55		von Bodungen et al., 1995
Norwegian Basin	NB	3350	500	70.0	-0.4	19.02.92	19.02.93	366	21.01	1.76		Peinert et al., 2000
Norwegian Basin		3350	1000	70.0	-0.4	19.02.92	19.02.93	366	21.63	2.31		Peinert et al., 2000
Norwegian Basin		3350	3000	70.0	-0.4	19.02.92	19.02.93	366	48.65	2.24		Peinert et al., 2000
Norwegian Basin		3350	3000	70.0	-0.4	20.02.87	21.02.88	366	41.54	2.96		von Bodungen et al., 1995
Lofoten Basin	LB	3160	2760	69.5	-10.0	31.07.83	14.07.84	349	22.00	1.34		Honjo et al., 1988
Voering Plateau	VP	1440	500	67.6	-5.8	23.03.87	22.03.88	365	30.73	3.46		von Bodungen et al., 1995
German JGOFS-L3	L3	3070	1000	54.0	21.0	29.07.95	03.07.96	340	27.31	4.43	38	Schulz-Bull et al., unpublished
German JGOFS-L3		3070	1000	54.0	21.0	20.03.96	22.03.97	367		1.15	38	Schulz-Bull et al., unpublished
German JGOFS-L3		3070	2200	54.0	21.0	20.03.94	20.03.95	365	18.67	0.57	77	Kuss and Kremling, 1999
German JGOFS-L3		3070	2200	54.0	21.0	21.03.95	22.03.96	367	22.77	2.13	77	Schulz-Bull et al., unpublished
German JGOFS-L3		3070	2200	54.0	21.0	20.03.96	22.03.97	367	15.34	0.65	77	Schulz-Bull et al., unpublished
OMEX 2	OX2	1500	600	49.6	12.3	01.07.93	01.07.94	365	18.95	2.10	38	Antia et al., 1999
OMEX 2		1500	1050	49.6	12.3	01.07.93	01.07.94	365	26.48	2.22		Antia et al., 1999

OMEX 3	OX3	3260	580	48.9	13.5	01.07.93	20.05.94	323	12.00	1.78	34	Antia et al., 1999
OMEX 3		3260	1440	48.9	13.5	01.07.93	01.07.94	365	42.50	3.61		Antia et al., 1999
OMEX 3		3260	3220	48.9	13.5	01.07.93	01.07.94	365	37.78	1.89		Antia et al., 1999
Honjo-48°N	48°N	4435	1000	48.0	21.0	03.04.89	02.04.90	364	20.70	1.48	41	Honjo & Manganini, 1993
Honjo-48°N		4435	1000	48.0	21.0	03.04.89	02.04.90	364	26.90	1.38		Honjo & Manganini, 1993
Honjo-48°N		4000	3300	48.0	21.0	03.04.89	02.04.90	364	26.90	1.00	103	Honjo & Manganini, 1993
BOFS-49°N	BOFS1	4555	3100	47.0	20.0	18.04.89	22.04.90	369	22.06	1.78	80	Newton et al., 1994
German JGOFS-L2	L2	4481	500	47.0	20.0	04.04.92	04.04.93	365	7.57	0.77	15	Fehner & Koeve, unpublished
German JGOFS-L2		4481	500	47.0	20.0	20.03.94	23.03.95	368	5.05	0.62	15	Fehner & Koeve, unpublished
German JGOFS-L2		4481	1000	47.0	20.0	28.03.92	28.03.93	365	11.21	1.20	20	Kuss and Kremling, 1999
German JGOFS-L2		4481	2000	47.0	20.0	20.03.94	20.03.95	365	24.37	0.90	54	Kuss and Kremling, 1999
German JGOFS-L2		4481	2000	47.0	20.0	23.03.95	24.03.96	367	23.27	1.25	54	Schulz-Bull et al., unpublished
German JGOFS-L2		4481	2000	47.0	20.0	17.03.96	19.03.97	367	20.11	1.33	54	Schulz-Bull et al., unpublished
German JGOFS-L2		4481	3500	47.0	20.0	28.03.92	28.03.93	365	15.34	0.65	64	Kuss and Kremling, 1999
Honjo-34°N	34°N	5172	1159	34.0	21.0	03.04.89	18.03.90	349	19.40	1.00	60	Honjo & Manganini, 1993
Honjo-34°N		5172	1981	34.0	21.0	03.04.89	18.03.90	349	22.40	1.03	90	Honjo & Manganini, 1993
Honjo-34°N		5172	4472	34.0	21.0	03.04.89	18.03.90	349	21.90	0.85	123	Honjo & Manganini, 1993
German JGOFS-L1	L1	5275	2000	33.1	22.0	12.03.94	14.03.95	367	13.34	0.62	52	Kuss and Kremling, 1999
German JGOFS-L1		5275	2000	33.1	22.0	14.03.95	16.03.96	368	15.78	0.70	52	Schulz-Bull et al., unpublished
German JGOFS-L1		5275	2000	33.1	22.0	20.03.96	23.03.97	368	15.18	0.80	52	Schulz-Bull et al., unpublished
German JGOFS-L1		5275	4000	33.1	22.0	18.10.93	02.09.94	319	18.41	0.67	71	Kuss and Kremling, 1999
Sargasso Sea	OFP	4400	500	31.8	64.2	17.11.84	18.11.85	366	12.83	2.25		*see legend
Sargasso Sea		4400	500	31.8	64.2	11.11.89	14.11.90	368	8.76	1.02		*see legend
Sargasso Sea		4400	500	31.8	64.2	13.12.90	03.12.91	355	14.79	1.42		*see legend
Sargasso Sea		4400	500	31.8	64.2	20.12.91	19.12.92	365	16.22	1.89		*see legend
Sargasso Sea		4400	1500	31.8	64.2	17.11.84	18.11.85	366	13.62	1.01		*see legend
Sargasso Sea		4400	1500	31.8	64.2	11.11.87	14.11.88	369	15.00	0.98		*see legend
Sargasso Sea		4400	1500	31.8	64.2	15.11.88	11.11.89	361	10.93	0.74		*see legend
Sargasso Sea		4400	1500	31.8	64.2	11.11.89	14.11.90	368	10.96	0.63		*see legend
Sargasso Sea		4400	1500	31.8	64.2	26.12.90	20.12.91	359	16.18	0.93		*see legend
Sargasso Sea		4400	1500	31.8	64.2	20.12.91	19.12.92	365	13.94	0.96		*see legend
Sargasso Sea		4400	3200	32.1	64.2	06.12.79	10.12.80	370	13.86	0.68		*see legend
Sargasso Sea		4400	3200	32.1	64.2	10.12.80	03.12.81	358	18.23	0.89		*see legend
Sargasso Sea		4400	3200	32.1	64.2	03.12.81	08.12.82	370	18.41	0.92		*see legend
Sargasso Sea		4400	3200	32.1	64.2	18.01.83	18.01.84	365	16.16	0.79		*see legend
Sargasso Sea		4400	3200	31.8	64.2	17.11.84	18.11.85	366	12.15	0.65		*see legend
Sargasso Sea		4400	3200	31.8	64.2	14.11.86	10.11.87	361	13.14	0.54		*see legend
Sargasso Sea		4400	3200	31.8	64.2	11.11.87	14.11.88	369	14.78	0.72		*see legend
Sargasso Sea		4400	3200	31.8	64.2	15.11.88	11.11.89	361	13.25	0.61		*see legend

Sargasso Sea		4400	3200	31.8	64.2	11.11.89	14.11.90	368	10.97	0.51	*see legend
Sargasso Sea		4400	3200	31.8	64.2	26.12.90	20.12.91	359	14.72	0.69	*see legend
Sargasso Sea		4400	3200	31.8	64.2	20.12.91	19.12.92	365	14.82	0.69	*see legend
Sargasso Sea		4400	3200	31.8	64.2	19.12.92	16.12.93	362	11.52	0.60	*see legend
Sargasso Sea		4400	3200	31.8	64.2	16.12.93	30.12.94	379	10.93	0.52	*see legend
Sargasso Sea		4400	3200	31.8	64.2	30.12.94	19.12.95	354	12.81	0.59	*see legend
Sargasso Sea		4400	3200	31.8	64.2	31.12.96	17.12.97	351	14.71		*see legend
Canary Islands	CI	3600	1000	29.0	15.5	25.11.91	24.11.92	365	6.43	0.48	Neuer et al., 1997
Canary Islands		3600	1000	29.0	15.5	06.08.92	06.08.93	364	10.83	0.86	Neuer et al., 1997
Canary Islands		3600	3000	29.0	15.5	25.11.91	24.11.92	365	17.24	0.81	Neuer et al., 1997
Canary Islands		3600	3000	29.0	15.5	27.11.92	27.11.93	365	18.76	0.87	Neuer et al., 1997
Canary Islands		3600	3000	29.0	15.5	06.05.93	06.05.94	365	15.58	0.77	Neuer et al., 1997
BOFS 2	BOFS2	4860	3870	24.6	22.8	14.10.90	27.09.91	348	15.14	0.73	Newton et al., 1994
EUMELI_M	EUM-M	3100	2500	21.0	31.0	11.02.87	06.01.88	329	74.75	7.68	Aloys and Bory, 2000
EUMELI_M		3100	3000	21.0	31.0	27.11.87	23.11.88	362	58.63	1.91	Aloys and Bory, 2000
EUMELI_O	EUM-O	4560	1000	18.0	21.0	17.02.87	15.02.88	363	11.48	0.61	Aloys and Bory, 2000
EUMELI_O		4560	2500	18.0	21.0	17.02.87	15.02.88	363	11.52	0.50	Aloys and Bory, 2000
Cap Blanc	CB	4094	730	21.1	20.7	19.11.90	19.11.91	365	31.02	3.76	Fischer et al., 2000
Cap Blanc		4094	3557	21.1	20.7	19.11.89	19.11.90	365	59.19	1.88	Wefer & Fischer, 1993
Cap Blanc		4094	3557	21.1	20.7	19.11.90	19.11.91	365	32.09	2.36	Fischer et al., 2000
Cap Blanc		3646	2195	20.8	19.8	22.03.88	22.03.89	365	67.17	2.74	Wefer & Fischer, 1993
Guinea Basin	GB	4522	859	1.8	11.1	04.04.90	07.04.91	368	30.60	2.94	Fischer et al., 2000
Guinea Basin		4522	3965	1.8	11.1	04.04.90	30.03.91	360	44.20	2.18	Fischer et al., 2000
Guinea Basin		4481	853	1.8	11.1	01.03.89	16.03.90	380	28.08	3.03	Wefer & Fischer, 1993
Guinea Basin		4481	3921	1.8	11.1	01.03.89	25.02.90	361	37.29	2.19	Wefer & Fischer, 1993
Guinea Basin		3912	696	-2.2	9.9	01.03.89	16.03.90	380	9.41	1.09	Wefer & Fischer, 1993
Walvis Ridge	WR	2196	599	-20.0	-9.2	18.03.89	13.03.90	360	48.78	5.07	Wefer & Fischer, 1993
Walvis Ridge		2217	1690	-20.0	-9.2	04.03.88	16.03.89	377	59.06	6.08	Wefer & Fischer, 1993
Walvis Ridge		2196	1648	-20.0	-9.2	18.03.89	13.03.90	360	37.44	3.83	Wefer & Fischer, 1993
Walvis Ridge		2196	1648	-20.0	-9.2	25.03.90	09.04.91	380	23.66	2.77	Fischer et al., 2000
Kerguelen Island	KI	1952	1588	-62.3	57.5	01.12.83	25.11.84	360	108.7	5.13	Wefer & Fischer, 1991
Kerguelen Island		1650	693	-62.3	57.5	14.06.84	14.06.85	365	25.90	0.71	Wefer & Fischer, 1992
Kerguelen Island		1992	687	-62.4	57.8	07.05.85	07.05.86	365	50.00	1.48	Wefer & Fischer, 1993
Weddel Sea	WS	5053	360	-64.9	2.6	16.01.88	15.01.89	365	35.24	3.49	Wefer & Fischer, 1994
Weddel Sea		5044	863	-64.9	2.6	25.01.85	25.01.86	365	0.26	0.03	Wefer & Fischer, 1995

[a] Trap efficiencies calculated based on ^{230}Th and ^{231}Pa budgets from Scholten et al., 2001

* Data were downloaded digitally from the Ocean Flux Programme Website (http://www.whoi.edu/science/MCG/ofp). For long-term analyses of these data refer to Deuser 1996 and Conte et al., (in press)

Missing values were interpolated for intervals of up to 2 weeks using the mean value of the neighbouring cups. Where gaps in the data occurred during low and constant flux (such as in winter) the mean value of that period from the entire data set was used if appropriate. The OFP time-series of particle flux in the deep western Sargasso Sea is the longest time-series of its kind and has produced a unique record of temporal variability in the "biological pump" (Deuser et al. 1982, Deuser 1986, Conte et al., 2001 and references therein). Horizontal currents in the area are low, averaging <5 cm sec^{-1} at 1500m (Siegel and Deuser, 1997), so aliasing of the flux record by hydrodynamic variables is thought to be minimal.

Annual Integrals: Since annual fluxes are used to quantify the relationship to surface productivity, care was taken to integrate over appropriate time periods. Often, annual fluxes are reported as the mean flux over a deployment period extrapolated to 365 days, or else as a cumulative year of flux from trap deployment to trap recovery. Since deployment and recovery at sea are, for logistical reasons, frequently during high flux periods in summer, this method has the error of assigning a proportion of the peak flux to one year, and another portion to the next. Here we integrate over deep mixing cycles (i.e. from winter to winter) since the nutrient budget, which determines annual new production, is set during deepest winter mixing. With some exceptions (see Table 1) integration was from Feb/March of one year (the time of deepest mixing in the North Atlantic) to the corresponding month of the following year. For sites in the southern hemisphere integration was from May/June to May/June of the following year wherever possible (Kerguelen Island). For the OFP data from the Sargasso Sea, annual integrals were taken from Nov./Dec of one year to the next, that corresponds to periods of lowest, least variable flux (Deuser, 1996) and productivity (Steinberg et al., 2001). During Feb./March, both flux and productivity are high and vary more between years. Particularly at sites where there is large seasonal variability in fluxes between years a comparison of these integration methods (over deployment periods vs. over mixing cycles) yields large differences. For example (Figure 2), at L2 (47°N, 20°W), annual fluxes over deep mixing cycles vary by 10 % around the mean (mean 22.6 ± 2.2 gDW $m^{-2}y^{-1}$) whereas they vary by 38 % around the mean (mean 20.1 ± 7.6 gDW $m^{-2}y^{-1}$) when integrated over deployment periods. Because of this potential bias, we have calculated annual fluxes over deep mixing cycles even though this has reduced the amount of data used. The resulting integrals in Table 1 may thus differ from those reported in the source publications.

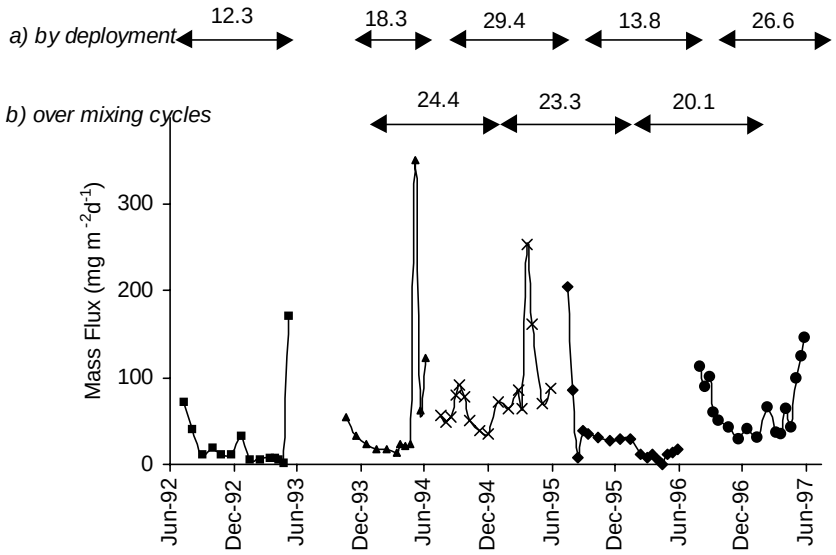

Figure 2: Long-term recordings of mass flux at 2000 m at station L2 (47°N, 20°W). Different symbols are data from consecutive deployments at the same site. Annual integrals are calculated by different means: a) by deployment period and b) over cycles of deep mixing (i.e. winter to winter)

Primary / New Production Estimates: The selection of primary production estimates also proves to be no trivial matter. We compared estimates from the models of Longhurst et al. (1995), Antoine et al. (1996) and Behrenfeld and Falkowski (1997) for individual stations. Values were taken for a 1° x 1° grid centred on the trap sites that is representative of the mean surface variability in hydrographical conditions where particles settling to the traps are produced. For comparison with new production and f-ratio estimates we use data from Oschlies and Garcon (1998).

Although there is general agreement among models in the regional distribution of primary production, there is considerable site-specific discrepancy in the absolute values, particularly in polar regions where the estimates of Longhurst et al., (1995) are unreasonably high compared with regional estimates from nutrient budgets and models (Rey, 1991; v. Bodungen et al., 1995). There is better agreement between Antoine et al. (1996) and Behrenfeld and Falkowski (1997) with the difference that the latter have higher estimates for the latitudinal bands between 30°-60°N and 30°-50°S, resulting in a higher basin-wide estimate of 13.3 GtC yr^{-1} compared to 9.64 GtC yr^{-1} by Antoine et al. (1996) for the area considered in this study. We use the data of Antoine et al., (1996) for better comparison with a number of recent publications (Fischer et al., 2000; Najjar and Keeling, 2000; Schlüter et al. 2000). For additional comparison with the OFP flux data in the Sargasso Sea we extracted primary production data from the BATS (Bermuda Atlantic Time-series Study) online database (http://www.bbsr.edu) and integrated values linearly for the time intervals given in Table 1.

Seasonality Index: We use an index for the seasonality/periodicity of flux as defined by Berger and Wefer (1990) and Lampitt and Antia (1997) and call it the Flux Stability Index (FSI) as in Lampitt and Antia (1997). The FSI is calculated by ranking the flux values according to their magnitude and plotting the accumulated flux against time. The time in days for half of the total annual flux to arrive at the sediment trap is read off the graph and is the value of the Flux Stability Index; low values thus indicate systems with highly pulsed export; high values indicate more constant sedimentation over time.

3. Results and Discussion

3.1. Efficiency of sediment traps

For the entire data set (n=105) there is no clear relationship of POC flux with trap depth (Figure 3a). For open ocean situations, without strong lateral sources of particles, POC fluxes must decrease with depth since the degradation rate of POC (range 3 d to 1 yr., Eppley et al., 1983; Lande and Wood, 1987) is rapid compared to known particle sinking rates. Even trap bypassing by swimmers or the differing collection funnel at the surface (Siegel and Deuser, 1997; Waniek et al., 2000) will merely affect the relative decrease of POC with depth and not cause its increase. For a number of stations however there is a decrease in flux above 1000 m, which may be a result of low collection efficiencies of the traps.

Although flux measured in deep traps in the Sargasso Sea were seen to agree well with estimates from ^{230}Th and ^{231}Pa budgets, (Bacon et al., 1985) shallow traps are notoriously poor in performance (Michaels et al., 1994; Buesseler et al., 2000). Buesseler (1991) found severe discrepancies (factor + 10 to –10) between expected and measured ^{234}Th fluxes in drifting traps at 20-150 m depth over periods of 3-20 days. Since shallow drifting traps are exposed to a different hydrodynamic environment than those moored at several hundred meters, it is unclear as to how these results may translate to deep, moored traps.

For a subset of the data (n=24) Scholten et al. (2001) show poor trapping efficiencies based on the expected annual fluxes of ^{230}Th. These range from under 50% (i.e. measured flux = 50% of expected flux) for traps shallower than 1000 m to between 64% and 123% for traps below 3000 m. Scaling the measured trap fluxes using these "correction" factors yields the expected decrease in POC and PON flux with depth (Figure 3b), though for a greatly reduced data set. Applying such a correction factor to the measured variables assumes that particle trapping efficiency is based on hydrodynamic effects that bias all components of flux equally (but see also Gust et al., 1994; Buesseler et al., 2000). For the trap correction

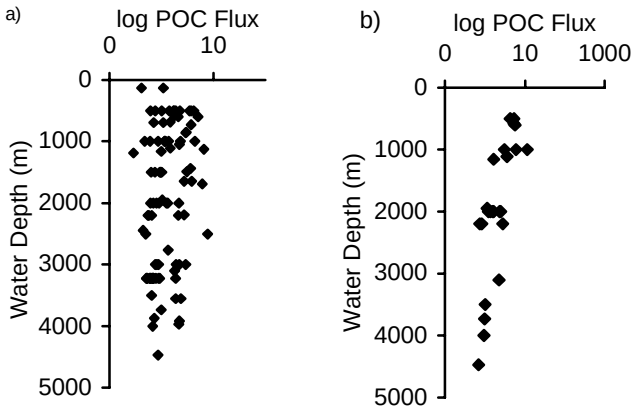

Figure 3: Relationship of particulate organic carbon (POC) flux to depth based on the entire data set in Table 1 without correction for ^{230}Th flux (a), and using ^{230}Th corrected data only (b)

factors used here we refer to a detailed discussion of their validity to Scholten et al. (2001), who find no clear relationships between ^{230}Th fluxes and those of specific variables, implying no discernible selectivity in trapping efficiency. We thus use the ^{230}Th correction for all components measured; because there is no consensus on this issue we present results from stations with and without ^{230}Th corrections separately.

3.2. Interannual variations in Flux

Since determination of empirical algorithms relating flux to production and water depth rely on annual means of productivity, we first examine to what extent interannual variations in flux can contribute to variations in export ratios.

Interannual variability in fluxes is difficult to determine given the short time period of most studies (excluding the Sargasso Sea station). Table 2 summarises the median values and variance of POC fluxes at single trap depths where at least 3 years of data are available.

Annual fluxes vary little at the more tropical, oligotrophic sites L1, Canary Islands and Sargasso Sea. The site Walvis Ridge is strongly influenced by the nearby lateral gradient in production from the adjacent coastal upwelling and the formation of "giant filaments" that can extend over the trap site in some years, causing large interannual variations (Fischer et al., 2000). At L3 the differences in annual fluxes between consecutive years is difficult to explain, and may be caused by horizontal advection of

particles from the nearby Rockall Plateau. Aside from WR and L3, annual variations are small compared to site-specific differences in flux.

Table 2: Median and variance of annual POC fluxes from sites where 3 or more years of data are available.

Site	Trap depth (m)	Median	Variance	n=
L3	2200	1.81	1.49	3
L2	2000	2.31	0.48	3
Canary Island	3000	0.81	0.003	3
L1	2000	1.35	0.03	3
Sargasso Sea	500	1.65	0.29	4
	1500	0.94	0.02	6
	3000	0.67	0.02	14
Walvis Ridge	1690	3.83	2.86	3

In Figure 4 we examine interannual variations in the depth dependency of the export ratio,

grouping sites L2 with 48°N and L1 with 34°N, since they were at the same location.

There is encouraging similarity in fluxes at a single site and differences between sites. The Sargasso Sea site is unique in that there are long-term primary production data with approximately monthly resolution available from the BATS (Bermuda Atlantic Time-series Study) program (Michaels and Knap, 1996; Steinberg et al., 2001) with which to compare annual variations in flux. The annual primary production at this site from the model estimate of Antoine et al., (1996) is 82.4 gC $m^{-2}y^{-1}$, compared to estimates from the BATS data of 130, 157 and 186 gC $m^{-2}y^{-1}$ for the years 1989-1990, 1990-1991 and 1991-1992 respectively (integrated over the time periods listed in Table 1). Variations in flux between these years reflects these changes in annual production, such that differences in export ratio between years based on a single model estimate (Figure 4b, left) are largely lost when using site-specific real-time data (Figure 4b, right). There are precious few sites for which such data is available, and these results point to an extremely tight coupling of production with flux over annual time scales. In summary, we conclude that although there are some interannual variations in flux and the extent to which it decreases with depth, these are smaller than the differences between sites, allowing inter-site comparisons based on the available data.

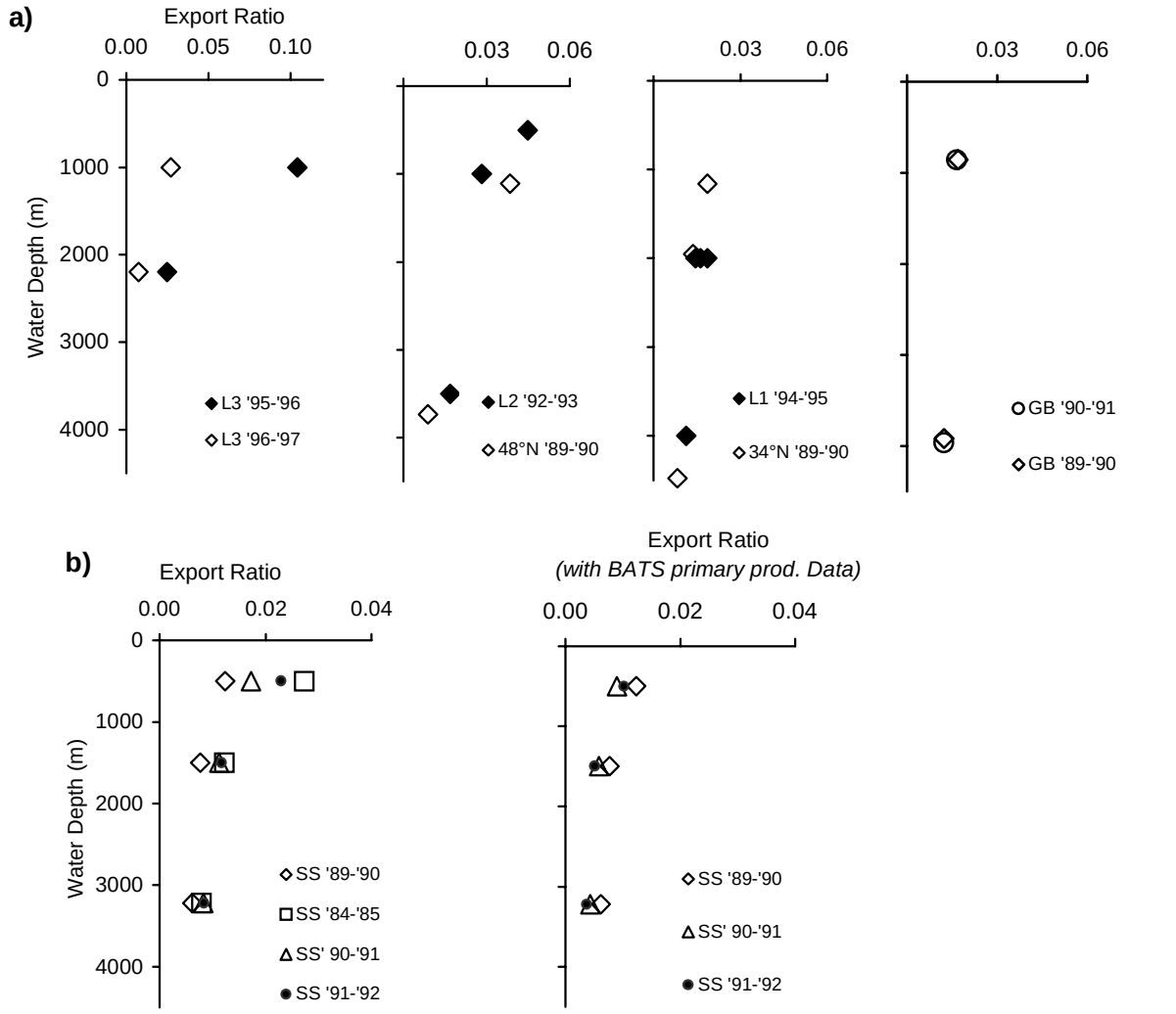

Figure 4: Changes in the Export Ratio (POC flux/ Primary Production) with depth at sites where data are available for more than one year. In 3b) data are plotted for the Sargasso Sea using model estimates of primary production from Antoine et al., (1996) at left, and using primary production estimates from the BATS site at right.

3.3. Relationship of Export Ratio to depth and Primary Production

By applying correction factors to account for low trapping efficiencies and in view of the generally low interannual variations in flux we proceed to examine regional and basin-wide relationships based on a reduced, but robust, data set.

For depth-dependant degradation of fluxes we apply the model

$$J_{Corg} = c^* PP^a * Z^b \quad (1)$$

as used by Betzer et al. (1984), to derive an algorithm relating flux to productivity and depth, where J_{Corg} is the organic carbon flux (gC $m^{-2}y^{-1}$) at depth Z (m), PP is primary production (gC $m^{-2}y^{-1}$) and a, b and c are constants. Data used for the fit are those with ^{230}Th correction only (n=24). This reduced database is distributed between 33°N and 54°N, representing a range of production from the oligotrophic gyre to the sub-polar north Atlantic.

Using Model II least squares regression, the best fit yields

$$J_{Corg} = 0.1 * PP^{1.77} * Z^{-0.68} \quad (1a)$$

$R^2 = 0.803$, n=24

The resulting curve is essentially similar to that of Berger et al., (1987) who used a global data compilation. The exponent of the depth term z (-0.68), that represents the curvature of fit, is similar to the empirically determined values of Betzer et al. (1984) and Pace et al. (1987) from the oligotrophic Pacific (0.63 and 0.734 respectively). Figure 5a shows the depth dependence of export ratio (ER) for these and other empirical algorithms (Suess, 1980; Betzer et al., 1984; Pace et al., 1987; Berger et al., 1987) calculated for a primary production value of 100 gC $m^{-2}y^{-1}$. Although basically the same in shape, there is a range in export ratio at 125 m from 0.12 (Pace et al., 1987) to 0.39 (Suess, 1980) depending on the algorithm used. The choice of algorithm and data on which it is based will thus have an impact on calculation of basin-wide export.

It is instructive to recall that the algorithms shown in Figure 5 are based on data from different sites and integrating over different periods. Although reported in units of flux per unit area and year (Suess, 1980; Betzer et al., 1984; Berger et al., 1987), these studies use short-term (days to weeks) measurements of flux and relate them to contemporaneous productivity integrated over the euphotic zone. Yet it is known that production and flux are not in balance on short time scales (Lohrenz et al., 1992) due to nutrient and particle retention by a seasonally variable food web (Wassmann 1998; Boyd a nd Ne wton 1999).

Use of any single algorithm, aside from yielding quantitative differences in export, implies that there is a globally applicable export ratio to a particular depth. However it has been demonstrated that regional differences in export ratio exist, and are related to the seasonality of export, with more pulsed export systems (typical for temperate and polar regions) exporting about twice as much of their production as systems with more constant export (typical for oligotrophic tropical systems) (Berger and Wefer, 1990; Lampitt and Antia, 1997). The low export ratio of Pace et al., (1997) for example, may thus reflect the oligotrophic conditions at the VERTEX site during their study and thus not be globally applicable.

Over steady state cycles, export at the base of the euphotic zone approximates new production (the fraction of primary production based on allochthonous nutrient sources; Eppley and Peterson, 1979). Over the range of primary production in the open ocean (50 – 300 gC $m^{-2}y^{-1}$) annually averaged f-ratios (the ratio of new to total production), range from <0.1 to ca. 0.5, and can be compared to the export ratio at 125 m (ER_{125}), the nominal depth of the euphotic zone. Variable f-ratios are an inherent feature of pelagic systems resulting from regional differences in physical forcing, degree and duration of stratification and degree of recycling by the pelagic food web. Assuming that export is linearly related to production (i.e. $PP^{1.0}$), implies that ER_{125} will remain constant for all values of PP, as is the case for the algorithms of Pace et al., (1987), Berger et al., (1987) and Suess (1980) (Figure 5b). The higher dependency on PP given by Betzer et al, (1987) ($PP^{1.41}$) and this study

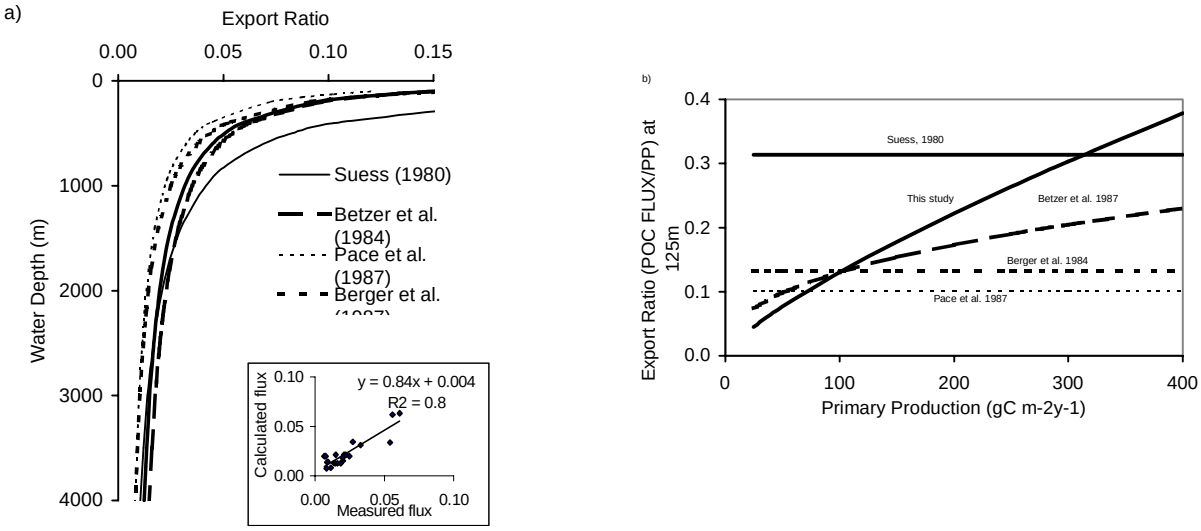

Figure 5: a) Relationship between Export Ratio and water depth using algorithms from the literature and from this study using ^{230}Th corrected data only. Insert: regression of measured flux at trap depth and calculated flux using the algorithm presented in this study. b) Changes in the Export Ratio calculated at a depth of 125 m using the algorithms presented in Figure 5a). $ER_{125} = c*PP^{a-1} * 125^{b}$; where a = 1, ER_{125} is thus constant

($PP^{1.77}$) yield corresponding changes in ER_{125} (and, by implication, f-ratios) from <0.1 to 0.23 and from <0.1 to 0.38 respectively over a range of PP from 50 to 400 gC $m^{-2}y^{-1}$. This is consistent with the early estimates of Dugdale and Goering (1967) and Eppley and Peterson (1979) and also with mean annual f-ratios estimated for oligotrophic and mesotrophic environments (Campbell and Aarup, 1992; Dugdale et al., 1992) by independent means. This is also in agreement with the increase in export ratio (normalised to 1000 m or 2000 m depth) with increasing primary production, as shown by Lampitt and Antia, (1997) and Fischer et al. (2000).

3.4. Regional differences in Export Ratio (ER) with depth

A main aim of this study was to examine regional differences in the efficiency of the biological pump. Previous studies have analysed such differences (Lampitt and Antia, 1997; Fischer et al., 2000) but have been unable to determine variations in the export function with depth, since data were normalised to a single depth.

A total of 10 stations in our data compilation have annual fluxes from 2 or more depths that allow a regional comparison. In Figure 6a changes in ER with depth for 5 stations based at 3 sites on a meridional transect at 20°W (33°N to 54°N) are presented, where data have been corrected by Scholten et al., (2001) using the ^{230}Th method. In Figure 6b and 6c a further 5 stations are compared where such a correction is not available.

For the ^{230}Th corrected data there is a clear latitudinal trend in variations of export ratio with depth. It is worth noting that the geographic locations of stations L1 and L2, (Kuss and Kremling, 1999) are identical to those of stations 34N and 48N (Honjo and Manganini, 1993) but were occupied during different years, using different moorings and methodology, yet cluster to show clear regional variations. The oligotrophic site at 33-34°N has a factor of 2 lower export ratio at 1000 m depth than the NABE site at 47-48°N. At 54°N (L3), there appears to be considerable interannual variability between the two successive years (1995 and 1996). This causes differences in the range of ER at L3, but both years show similar strong depth-dependant flux losses. As we show below, these differences between sites are also reflected in the composition of sedimenting particles and the seasonality index, giving us some confidence in interpretation of site – specific differences.

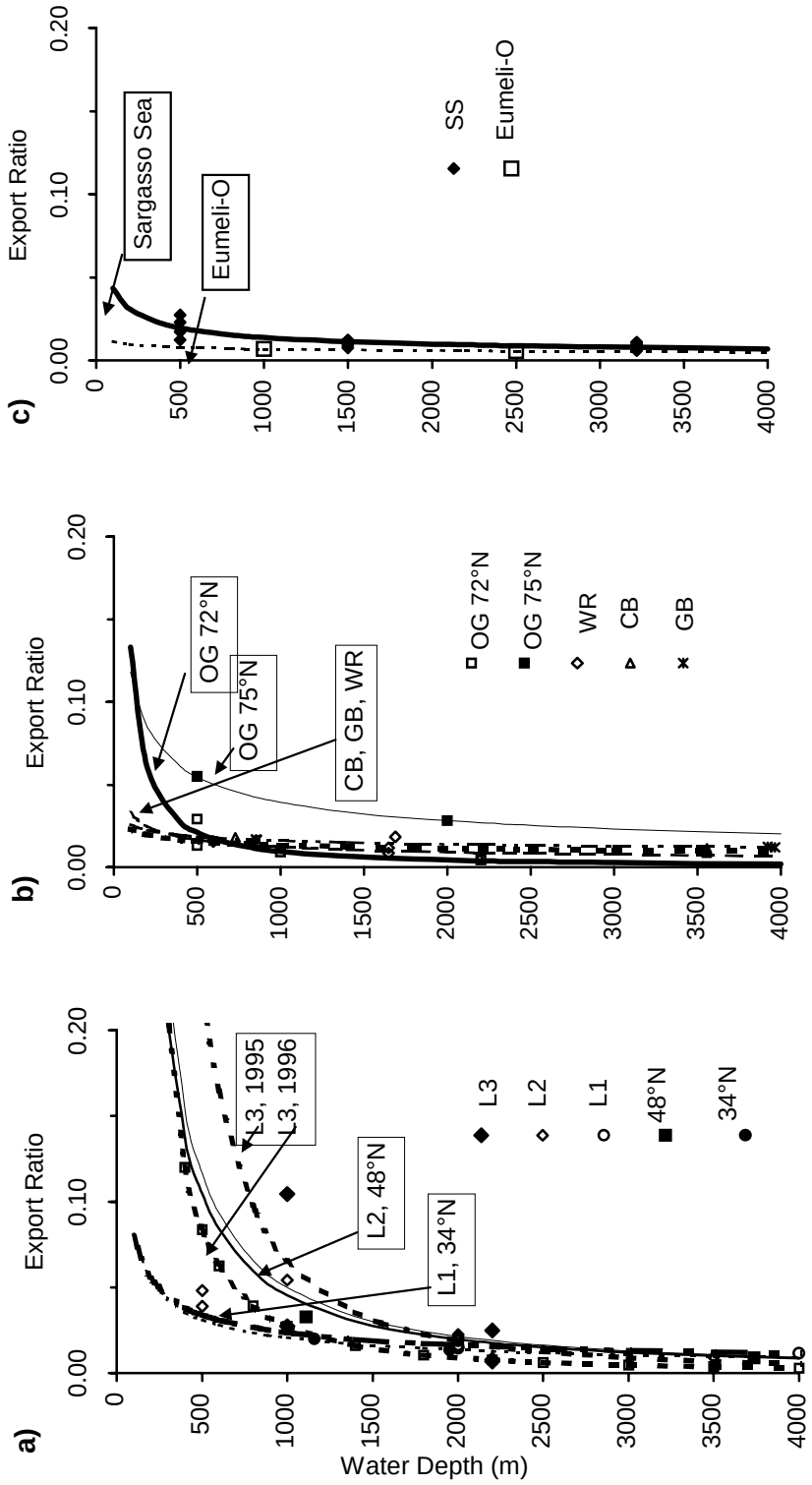

Figure 6: Changes in Export Ratio with water depth at individual sites. Lines are regressions through the data as per equation 1 in text. Data from 500 m at L2 have not been used for the regression

Figures 6b and 6c show data from sites where ^{230}Th correction is not available. On the basis of the ER and depth-dependant degradation rates these can be roughly grouped in three clusters; 2 sites in the East Greenland Sea (OG and OG 75°N), 4 sites in the subtropical Atlantic (Guinea Basin, Cap Blanc, Walvis

Ridge and the Sargasso Sea) and one site in the oligotrophic N. Atlantic gyre (EUMELI-O). The OG 75°N site experiences seasonal ice coverage where the growth period is limited to a few months a year – here we see maximum export ratios. This is probably due to the most rapid transfer of particles to depth that is characteristic for ice margin conditions where grazing is low, and particle export can be rapid. The open ocean site OG at 72°N also has high export ratio above 500 m, with a sharp decrease to 2000 m. The second group of sites in the subtropical Atlantic show low export ratios and little flux degradation with depth – export ratios are uniformly below 0.02 (as reported by Fischer et al., 2000). The most oligotrophic site in the subtropical N. Atlantic gyre (EUMELI-O) shows the lowest ERs encountered (0.07 and 0.056 at 1000 m and 2500 m respectively).

3.5.Comparison of Export Production to New Production

A major concern in extrapolating fluxes measured well below the euphotic zone (≥ 500m) to a depth of 125 m is that most of the organic carbon degradation occurs between these depth horizons. Essentially, all algorithms including ours have the weakness that they use relatively small variations in flux at greater depths to extrapolate to larger variations near the surface. We thus find it instructive to compare the algorithm presented here to modelled new production estimates that do not share this caveat.

Extrapolating measured differences in the export function with depth upward to the base of the euphotic zone shows clear regional differences in export (new) production. We have fitted the flux function (Equation 1) to the regional data to extrapolate to ER at 125 m [ER_{125}, approx. the euphotic depth used by Oschlies and Garcon (1998) to calculate new production]. The resulting curves are statistically weak, based as they are on so few data points and the curvature is largely determined by the relatively small variation in ER ≥ 500m. Nonetheless, we compare the ER_{125} to f-ratio at the same depth using model estimates of new production (Oschlies and Garcon, 1999) and total production (Antoine et al., 1996). With the exception of data from the Sargasso Sea, there is good agreement between the estimates (Figure 7a). The Sargasso Sea site lies near the strong gradient in new production at the north-western edge of the subtropical gyre, with higher new production than in the gyre itself. New production estimates for this site of 0.33 molN $m^{-2}y^{-1}$ (Altabet, 1989), 0.56 molN $m^{-2}y^{-1}$ (Jenkins, 1988) and 0.50 molN $m^{-2}y^{-1}$, Oschlies and Garcon, 1999), are an order of magnitude higher than the 0.04 molN $m^{-2}y^{-1}$ extrapolated from the trap data. At the nearby BATS site, Lohrenz et al. (1992) estimate new production at 0.1 – 0.11 molN $m^{-2}y^{-1}$ from export to shallow (125 m) drifting sediment traps (but note large collection biases at these depths from Buesseler, 1991).

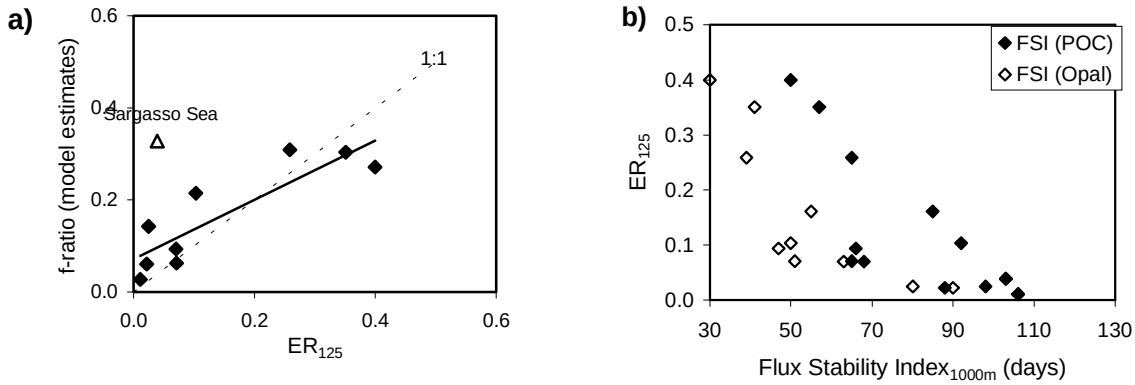

Figure 7:a) Comparison of Export Ratio at 125 m (ER_{125}) using ^{230}Th corrected data only with f-ratio using New Production estimates of Oschlies and Garcon, (1996) and Primary Production of Antoine et al. (1996). Least squares regression yields y = 0.65x +0.07, r^2 = 0.76, n=9. The Sargasso Sea was not included in the regression. b) Relationship of ER_{125} to Flux Stability Index based on POC and opal

fluxes. FSI has been normalised to 1000 m using regressions based on the entire data set. Low FSI values indicate pulsed export, high values more constant export with time

High new production/export systems are characteristic of high-latitudes, where the pelagic community is often dominated by bloom-forming plankton such as diatoms. Such bloom-and-bust scenarios have pulsed export and a strong seasonality in flux; this is seen in the strong correlation between the Flux Seasonality Index (FSI), export ratio (ER_{125}) and the rate of degradation of POC with depth (the z-exponent of equation 1) (Figure 6). Contrary to what is seen on the short time scales of such pulses, where a pulse of material can rapidly reach the sea bed (Lampitt, 1985), on an annual time scale high export systems do not provide proportionally more material to the deep-sea.

Despite large differences in shallow fluxes (by a factor of 24, from 0.5 – 11.65 gC $m^{-2}y^{-1}$), below 3000 m there is much less variation between sites (by a factor of 4.4, from 0.5 – 2.4 gC $m^{-2}y^{-1}$). This implies the presence of an active and efficient mid-water community, capable of and adapted to feeding on sinking particles till some minimal, threshold value of particles is reached that ultimately settle to the abyssal sea bed. This underscores the importance of this "twilight zone" (the depth horizon between the bottom of the euphotic zone and about 2000 m) that dampens the quantitative relationship between surface productivity and deposition to the sea floor. The 4-fold regional difference in deep-ocean fluxes reported here is of the same range as deep-sea benthic flux patterns (Jahnke, 1996). Both in their quantitative and marker signals, benthic fluxes and their accumulation in the sediments harbour valuable proxies that are used to reconstruct paleoproductivity scenarios (Sarnthein et al., 1992; Wefer et al., 1999).

3.6. Regional characteristics of export and composition of sinking particles

Regional characteristics based on the analyses above are still potentially influenced by methodological biases. We therefore make another comparison based on the composition of sedimenting particles, by conducting Principal Component Analyses (PCA) on the DW-normalised POC, PON, opal and carbonate fluxes (i.e. fluxes expressed as a fraction of DW flux) for the entire data set. The PCA is a technique of linear statistical predictors that has been widely applied in environmental sciences (Jackson, 1991). All statistical calculations were made by log-transformed data to improve the homogeneity of variance. The first two principal components span a two dimensional plane onto which each point can be projected. The plane is chosen in such a way that the variance of these projections is as large as possible. The position of each projected point on this plane can be visualised in the form of a so called biplot (Figure 8). The biplot shows the correlation between each mooring and the first two principal components by means of a vector. The length of each vector is equivalent to the fraction of the total variance that is explained the first two Principal Components.; thus all the variance in the concentration is explained by the first two Principal Components when a vector reaches the drawn unit circle.

Based on the temporal mode and depth dependency of flux (Figure 8a) sites geographically close to each other are similar and cluster separately from other groups of sites. Grouping of L1 with 34°N and L2 with 48°N is evident as is also the commonality between equatorial sites Cap Blanc and Guinea Basin and sites in the oligotrophic Equatorial N. Atlantic Gyre (Sargasso Sea and Eumeli_O). The polar OG 75°N site, under seasonal ice cover, and OG in the open Greenland Sea at 72°N are dissimilar with respect to export characteristics, primarily due to the low z-exponent at OG 75°N. This provides a first step towards the approach of defining geographical provinces according to their characteristics of the biological pump, however the spatial coverage of data is too weak to allow delineation in the form of biogeochemical provinces as described by Longhurst (1998).

Based on flux composition (Figure 8b) there is a clear clustering of sites with polar regions distinguished from non-polar by their high opal (mean 27% DW, range 5.2 – 45%) and low carbonate (mean 11.7% DW, range 4.8 – 21%) content. Outside of polar regions opal accounts for less than 10% (with the exception of the

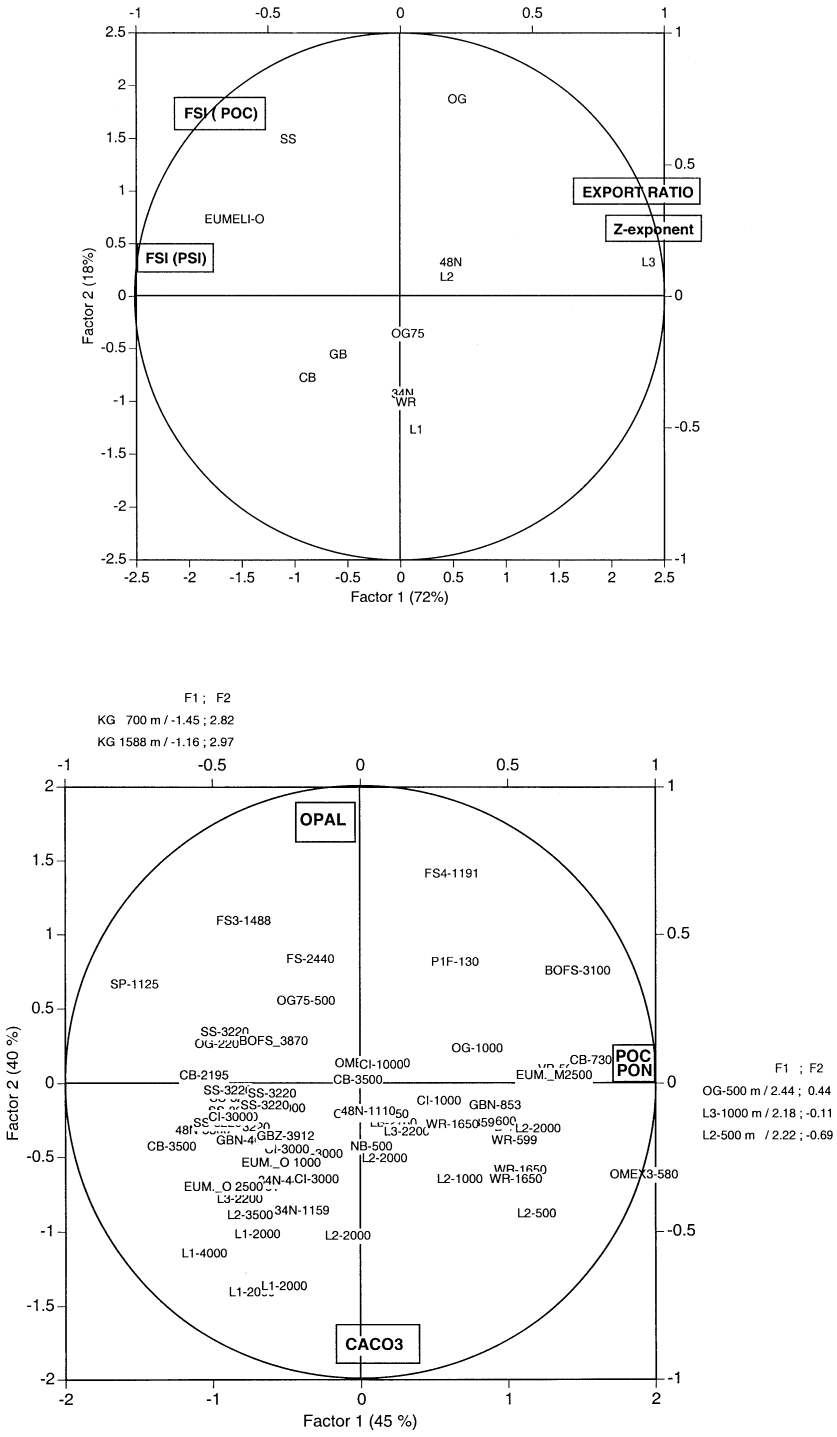

Figure 8: Principal Component Analysis based on a,(top) the characteristics of flux (Export Ratio, Flux Stability Index and value of the depth- exponent of z in equation 1(see text) and b, (bottom) based on the DW-normalised fluxes of POC, PON, carbonate and opal in sedimenting particles

Sargasso Sea at 13.7%) and carbonate for over 50% of sedimenting matter. As expected, highest opal content (45% DW) is seen in the Southern Ocean (KG) whereas in the Arctic Atlantic (FS, PI, OG75°N) this ranges from 5.7 to 14% DW.

Along a transect at 20°W in the eastern North Atlantic, stations L3, L2 and L1 show a

progressive decrease in opal: carbonate ratios going from North to South (Kuß and Kremling, 1999). The lack of cohesion in traps at different depths from L3 and L2 reflects differences in POC content from above 10% above 1000 m to below 5% at depths >2000 m. Interestingly, there is a difference in composition of flux between the mooring sites 48°N and L2 and 34°N and L1, that otherwise show strong similarity in flux characteristics (Figure 8a). We compare the opal:carbonate ratio in sedimenting material below 1000 m for the time period between 1989, when the moorings 34N and 48N were deployed, and the period between 1994-1997, when L2 and L1 were deployed at the same sites. There is a clear decrease in opal:carbonate ratios during this 8-year period, that is similar to the decrease in this ratio shown by Deuser et al., (1995) in the Sargasso Sea between 1978 and 1991 (Figure 9). Deuser et al., (1995) attempt to relate this to long-term changes in wind speed, implying that it may be a response to regional climatic variations. If the phenomenon is common to a larger area of the North Atlantic this may implicate some common cause related to large-scale physical forcing perhaps tied to the North Atlantic Oscillation. It is worth noting that, as reported by Deuser et al., (1995), the alteration in opal:carbonate ratios is primarily due to a drop in opal fluxes (50%)rather than an increase in carbonate flux (17%).

At 2000 m depth similar POC fluxes are registered, but POC:PIC ratios drop by 7 and 17% between 1989 and 1996 at 48°N and 34°N respectively. The decrease in opal fluxes are thus accompanied by decreased POC flux and lower efficiency of sequestration through alteration of the rain ratio of sedimenting particles. True time-series measurements in the ocean are rare, yet if the pattern seen in this study reflects a general change in structure of the pelagic community resulting from changes in physical forcing at the surface the implications are that changing surface mixing will change not just the absolute level of new production and thus export, but also the efficiency with which the biological pump exports to depth, providing a feedback mechanism to climate change.

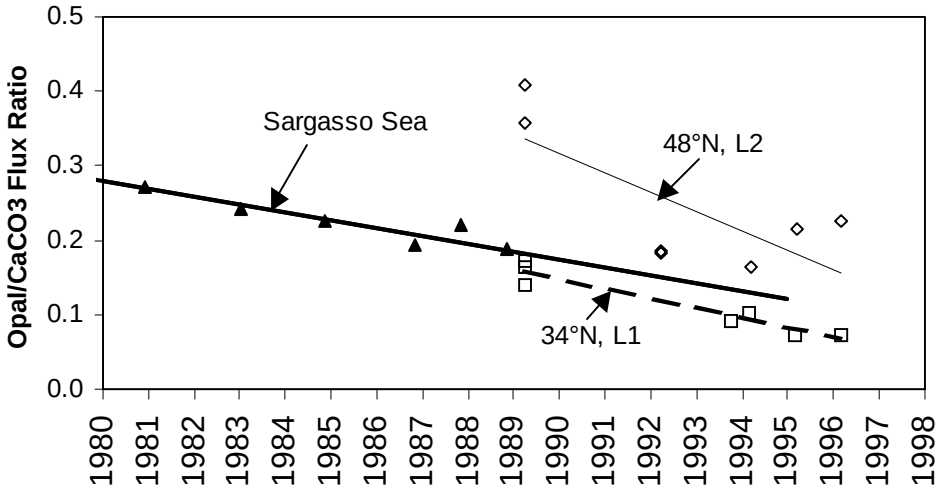

Figure 9: Long-term trend in the Opal: Carbonate ratio in sedimenting particles from the Sargasso Sea, at 47°N 20°W and from 34°N, 21°W. The line for the Sargasso Sea represents that derived by Deuser et al., (1995) with a slope of 0.0105 yr^{-1}. The slope of the lines for 48°N/L2 and 34°N/L1 are 0.026 yr^{-1} and 0.015 yr^{-1}respectively

3.7. Rain ratio

Since one of the aims of this study is to derive an estimate of basin-wide export flux as it is related to draw-down of atmospheric CO_2 by the biological (tissue and carbonate) pump, we examine regional and depth-related changes in the ratio of organic to inorganic carbon exported (POC:PIC, rain ratio, RR). Photosynthesis decreases the pCO_2 of surface waters, whereas calcite production increases pCO_2. During calcite production alkalinity is decreased, altering the carbonate equilibrium

of seawater such that at a molar POC:PIC ratio of 0.6:1 there is no net change in pCO_2 (Kano, 1990). Within the upper ocean this ratio differs spatially, both horizontally (regionally) and vertically, with photosynthesis exclusively within the euphotic zone and carbonate produced also by deeper-living zooplankton. Additionally, there is substantial and differential degradation of both POC and calcite within the upper 1000 m of the water column (see Figure 5; Milliman et al., 1999), that changes the ratio of POC:PIC in sinking particles.

Highest, and variable rain ratios are seen at polar sites and at continental margins (Figure 10a). Outside these regions, for the non-polar, open ocean data there is a good correlation of rain ratio with depth

$$POC:PIC = 7.79 - 0.89*Ln(Z) \quad r^2 = 0.72, n= 84 \qquad (2)$$

where POC:PIC is the rain ratio at water depth Z (in m). This gives a mean rain ratio of 3.7 at 125m. Significantly higher rain ratios from the polar oceans and continental margins underscore their importance in the global carbon cycle, since they are able more efficiently to sequester CO_2 for each unit of organic carbon produced.

Within the non-polar open ocean, and within the scatter of the data used to determine equation 2, there is a weak latitudinal trend of higher rain ratio at higher latitudes. These high latitude areas, which have higher export ratios and more pulsed export (Figure 10b) are more efficient net carbon exporting systems than the low-latitude systems. The ultimate gradient in pCO_2 between the surface ocean and atmosphere that can be equilibrated through gas exchange must take the rain ratio into account at the depth to which surface waters are exposed to contact with the atmosphere, namely the depth of maximal winter mixing.

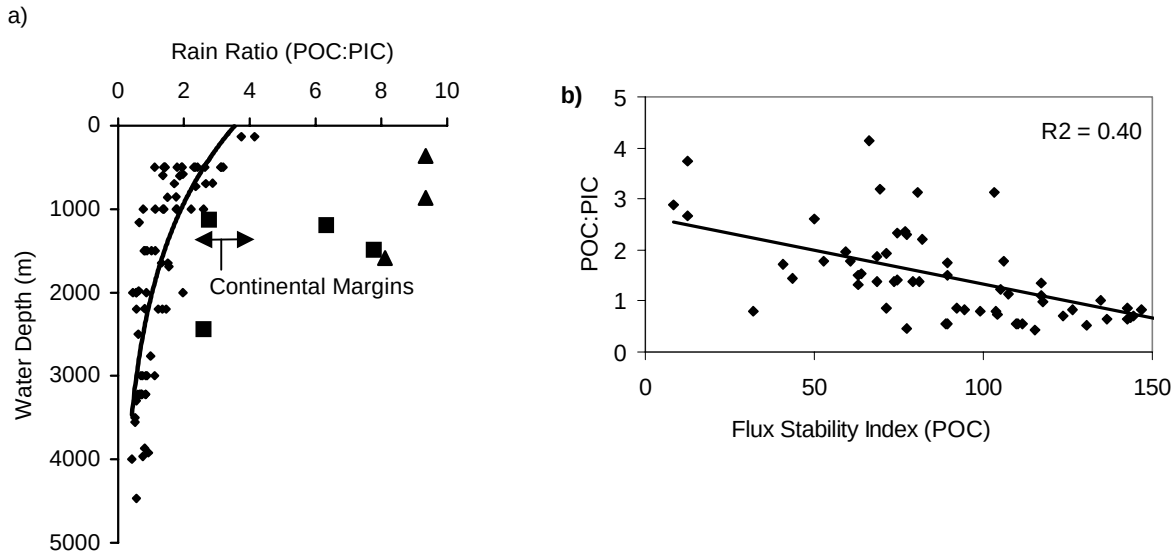

Figure 10: a) Changes in Rain Ratio (POC:PIC in sedimenting particles) with depth. The least squares regression (see text) is based on non-polar data only (diamonds). The Polar Arctic (squares) and Polar Antarctic (triangles) regions are shown separately. The arrows indicate the range of rain ratio in mid-water depths at Atlantic continental margins as summarised by Antia et al., (1999). b) Relationship of rain ratio to Flux Stability Index based on POC fluxes.

We estimate the net effect on surface seawater pCO_2 by the opposing processes of organic and inorganic carbon export at the mixed layer depth that we term the "Effective Carbon Flux", defined as the carbon export (accounting for the rain ratio) at the winter mixed layer depth that drives a potential draw-down of CO_2 from the atmosphere to the ocean:

$$J_{eff} = J_{POC} * [(RR-0.6)/RR] \quad (3)$$

where J_{eff} is the effective carbon flux, J_{POC} is the POC flux calculated according to equation (1a) to the WML depth, RR is the rain ratio at the WML depth, calculated according to equation (2) and 0.6 is the RR at which $\Delta pCO_2 = 0$. An obvious effect of the variations in rain ratio with depth is that the difference between J_{Corg} and J_{eff} widens with increasing water depth. Calculated immediately below the euphotic zone, at a nominal depth of 100 m, J_{eff} amounts to 84% of J_{Corg}; at 600 m depth the effective carbon flux is reduced to 71% of J_{Corg} , reflecting the increase in the carbonate fraction of export with depth. As a consequence, the quantitative sequestration flux is highest at low latitudes where maximal annual mixing is shallow, even though the "efficiency" of export, through higher rain ratios, is larger at higher latitudes. Changes in the depth of maximal ventilation will thus have multiple effects on the biological export of carbon: shoaling of the maximum mixed layer depth will cause a strong exponential increase in export ratio (Figure 5) as well as a smaller increase in net sequestration due to higher rain ratios. These will be counteracted by decreased nutrient inputs and decreased net production.

3.8. Basin-wide Flux Calculation

We next calculate carbon Fluxes for the Atlantic Ocean between 65°N and 65°S and 100°W and 20°E, with a resolution of 1° x 1°, excluding marginal Seas (the Baltic and Mediterranean Seas and the Hudson Bay). The total area of integration is 8.32 10^{13} m^2 , note, however, that the areas applies in estimating individual fluxes differ slightly depending on the availability of input data (see Table 3). A further assumption was made to account for the continental margins where the WML depth impinges on the slope. These areas are characterised by high productivity due to topographically induced upwelling; however, the majority of export production is remineralised on the shelf and upper slope does not contribute to long-term sequestration of carbon (Antia et al., 1999). We thus take as the continental boundaries of our calculations the slope depth to the depth of maximum winter mixing.

Table 3: Carbon Fluxes in the Atlantic Ocean.

	GT yr^{-1}	Area (* 10^{13} m^2)
PP	*9.64* [a]	
J_{125}	***1.68***	*8.32*
J_{WML}	***2.94***	*8.28*
J_{exp}	***3.14***	*8.32*
$R_{EXP-WML}$	*0.18*	*(8.32)*
J_{eff}	*2.47*	*8.26*

PP: primary production from Antoine et al., (1996)
J_{125}: POC flux calculated to a depth of 125 m as per equation 1b
J_{WML}: POC flux at the maximum depth of the winter mixed layer
J_{exp}: The maximal value of J_{125} and J_{WML} when the mixed layer depth is shallower than 125 m
$R_{EXP-WML}$: Remineralisation between the productive surface layer and the winter mixed layer depth
J_{eff} : effective carbon flux as defined in text and calculated according to equation 3

[a] *Antoine et al., (1996) estimate the integrated primary production of the Atlantic to be 9.86 GT C yr^{-1} (27% of their global primary production of 36.5 Gt C yr^{-1}). Their estimate is based on a slightly different regional definition of the Atlantic Ocean as compared to the one used in our study.*

Input data consist of annual primary production (Antoine et al., 1996) and maximum mixed layer depths from monthly resolved data based on climatological temperature and salinity data (Monterey and Levitus, 1997). The mixed layer depth is defined as the change in density with respect to the surface by 0.125 kg m^{-3}.

Results of basin-wide flux estimates are given in Table 3. J_{125} is the particle export flux calculated using equation (1b) at a depth of 125 m. J_{WML} is the corresponding flux at Z_{WML}, the maximum depth of the mixed layer. In the tropics, Z_{WML} becomes shallower than 125 m, hence a property J_{exp} is estimated as the maximal value of J_{125} and J_{WML} [J_{exp} = max (J_{125}, J_{WML})]. The remineralisation between the productive layer [min(Z_{WML}, 125)] and Z_{WML}, $R_{EXP\text{-}WML}$, is estimated from areal integrations of J_{exp} and J_{WML} to avoid errors due to slightly different areas on which these were based:

$$R_{EXP\text{-}WML} = (\Sigma J_{exp}/A_{exp} - \Sigma J_{WML}/A_{WML})*A_{WML}$$

where A_{exp} and A_{WML} are the areas for which J_{exp} and J_{WML} were calculated.

J_{eff}, the "effective" carbon flux, is calculated according to equation (3).

Figure 11 shows the resulting basin-wide flux calculations from 65°N to 65°S. Over this area total primary production is 9.64 GtC yr^{-1}, and J_{exp} amounts to 3.14 GtC yr^{-1} or a mean export (f-) ratio of 0.33 (Table 3). This value lies between the mean global f-ratio applying the Eppley and Peterson curve to estimates of primary production (mean f-ratio 0.3, Falkowski et al., 1998) and that from the eddy-permitting North Atlantic model of Oschlies & Garcon (1999) (f-ratio 0.43 between 8°S and 65°N). Export production of 3.14 GtC yr^{-1} for the area considered is however, over-proportionally large compared to the spring-summer global new production estimates based on net air-sea O_2 flux (4.5 – 5.6 GtC yr^{-1} globally, Najjar and Keeling, 2000). The basin-wide Effective Carbon Flux amounts to 2.47 GtC yr^{-1}.

The regional distribution of J_{exp} (Figure 11a) depicts high latitudes having a mean export (new) production about 10 times higher than the oligotrophic gyres. This pattern changes dramatically in terms of the effective carbon flux J_{eff} (Figure 11b), where the effects of regional variations in depth of winter mixing and changes in the rain ratio with depth are incorporated. Due to the high rain ration at shallow winter mixed layers (i.e. when WML ≈ 125 m), such as in the tropics, $J_{exp} \approx J_{eff}$ in these regions. In a global budget, the sequestration flux due to particulate export must be balanced against the outgassing of CO_2 from deep, upwelled water. The net effect of changes in upwelling intensity on the air-sea exchange of CO_2 through simultaneous changes in nutrient input, maximal ventilation and J_{eff} is largely unclear. In the subtropical and temperate Atlantic, deep mixing substantially lowers the effective carbon flux; low rain ratios at depth also contribute to a further decrease. In the context of the role of the biological pump in carbon sequestration it is, additionally, intuitively clear that small changes in depths of maximal mixing in the tropics will have a larger effect than corresponding changes at high latitudes.

The major features of Figure 11, depicting highest fluxes in regions of equatorial upwelling and at the continental margins, are similar to the patterns of benthic flux reported by Jahnke (1996). Locally, and on shorter time scales however, this pattern may vary considerably from the annual mean as a result of topographic effects on the seabed and the effects of short, rapid pulses of detrital input to the sea bed (Lampitt, 1985). Remineralisation above the winter mixed layer, $R_{EXP\text{-}WML}$, amounts to 0.19 GtC yr^{-1}, or 5.7 % of J_{exp}. This represents the fraction of export production that is not sequestered from contact with the atmosphere for climatically relevant time scales. This estimate is a minimal figure, since polar and sub-polar regions, where winter mixing is deepest, are excluded from our analysis.

A comparison of J_{eff} (Figure 11b) with primary production shows the importance of tropical upwelling regions, as a result of shallow winter mixed layers and high export fluxes (and f-ratios). These regions have a large contribution to basin-wide export flux, whereas the spring bloom areas of the North Atlantic are of secondary importance. The effect of calcite

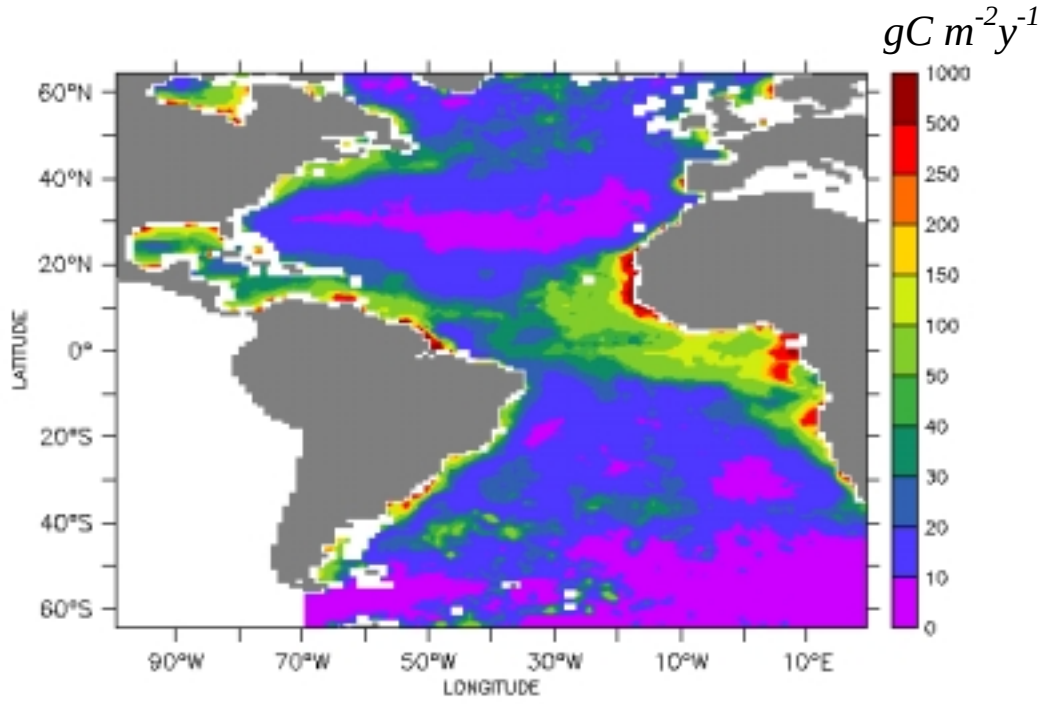

Figure 11: a (above) J_{exp}, the export flux, as defined in text [J_{exp} = max (J_{125}, J_{WML})], where $J_{125}$and J_{WML} are the POC fluxes at 125 m and the winter mixed layer respectively. b (below) J_{eff}, the "effective carbon flux" at the base of the winter mixed layer, calculated as per equation 3 in text

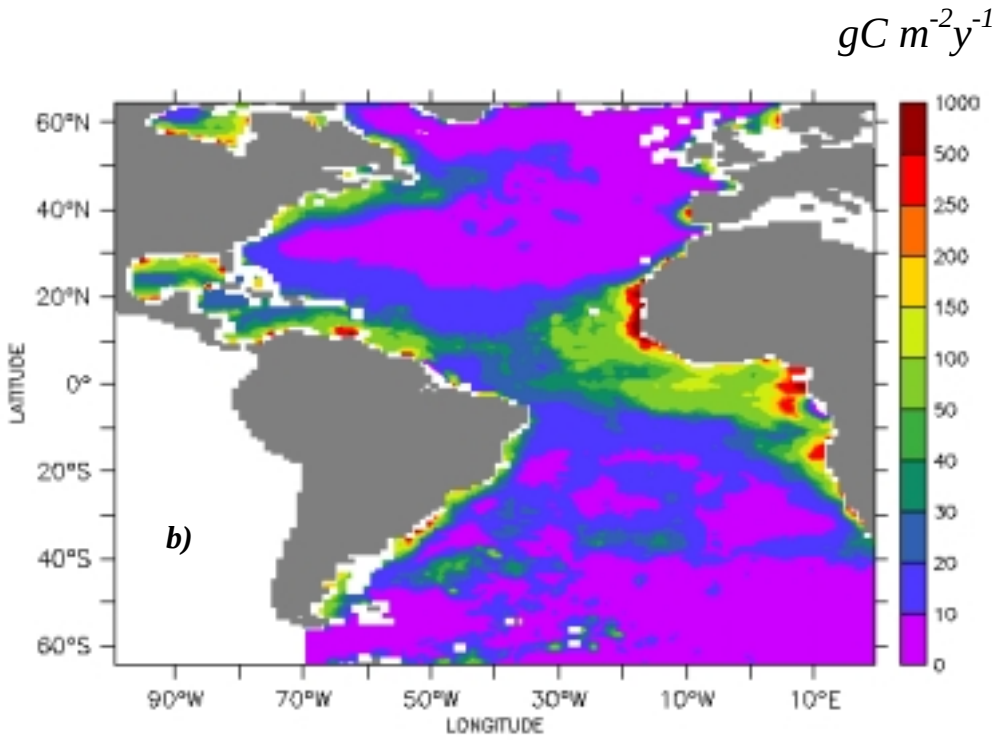

fluxes on the Effective Carbon Flux is greatest for the latitudinal bands north of 40°N and south of 30°S, where rain ratios of about 2 at the (deep) WML are significantly lower than RR of 4 – 5.5 at the (shallow) WML depths in the oligotrophic equatorial Atlantic. This leads to a further enhancement of the tropical upwelling regions in basin-wide export, and a further diminishing of the importance of the temperate bloom areas.

3.9. Feedbacks to climate

As has been pointed out by Smith and Mackenzie (1991) the mere functioning of an oceanic biological pump is not sufficient to alter atmospheric CO_2 levels or respond to anthropogenic CO_2 increase unless one of two conditions are met; a change in the efficiency of stripping available nutrients or an increase in availability and use of nutrients from land run-off. As discussed here, the effective carbon fluxes from the biological pump can vary as a function of changes in ventilation depth and rain ratio that are independent of these conditions. Projected changes in wind driven mixing in the temperate North Atlantic, aside from altering nutrient availability and thus the absolute levels of export production, will change the *efficiency* of sequestration by the combined effect of shallower ventilation (and thus equilibration with the atmosphere) and the higher rain ratio. Additional changes due to a shift from opal to carbonate producing organisms will have a negative feedback, lowering sequestration efficiency.

4. Conclusions

- The collection efficiency of sediment traps can be a major problem in empirical determination of export ratios and should be routinely included in further particle flux studies

- An empirical algorithm based on ^{230}Th corrected data yields differences in export (f-) ratio at 125 m of between 0.1 and 0.37 over a range of Primary Production between 50 and 400 gC $m^{-2}y^{-1}$.

- There are significant regional differences both in export at the base of the euphotic zone as well as the function describing POC degradation with depth, that are reflected in regional differences in flux seasonality and composition of sedimenting particles.

- Interannual variations in primary production, for which data are available for only one station, show corresponding differences in annual POC flux.

- Large differences in shallow fluxes are no longer visible below 3000 m, pointing to the importance of the twilight zone (200 – 2000m) in remineralising sinking organic particles to a threshold value

- Effective Carbon Flux, defined as that flux causing a potential sequestration of CO_2 from the atmosphere, is calculated using organic carbon fluxes and rain ratios (POC:PIC) at the base of the euphotic zone.

- Tropical upwelling regions are potentially major sequestration centres of carbon due to the combined effect of shallow winter ventilation and high rain ratios at the winter mixed layer depth

- 5.7 % of export flux at the base of the euphotic zone is remineralised above the winter mixed layer between 65°N and 65°S

Acknowledgements*:*

We thank Aloys Bory for providing us data from the EUMELI site in digital form, and Andreas Oschlies for providing new production estimates. We are grateful to Hugh Ducklow and 2 anonymous referees whose comments contributed to improvements in the manuscript. The time-series data that go into this analysis were collected by a large number of unnamed people over many years – without their continued and dedicated work, a synopsis of the kind presented here would not have been possible. The Ocean Flux Program time-series has been supported by the U.S. National Science Foundation since its inception. This publication is part of the German JGOFS Synopsis funded by the Bundesminister für Bildung, Forschung und Technologie (Bmb+f) and the Deutsche Forschungsgemeinschaft (DFG).

References:

Altabet, M.A. , Particulate new nitrogen fluxes in the Sargasso Sea, *J.Geophys.Res., 94*, 12771-12779, 1989

Antia, A.N., B. von Bodungen, and R. Peinert, Particle Flux across the mid-European continental margin. *Deep-Sea Res., 46*, 1999-2024, 1999

Antoine, D., J-M. Andre, and A. Morel, Oceanic primary production 2. Estimation at global scale from satellite (coastal zone color scanner) chlorophyll, *Global Biogeochem. Cycles, 10*, 57-69, 1996

Archer, D., and E. Meier-Reimer, Effect of deep-sea sedimentary calcite preservation on atmospheric CO_2 concentration, *Nature, 367*, 260-263, 1994

Bacon, M.P., C.A. Huh, A.P. Fleer, and W. Deuser, Seasonality in the flux of natural radionuclides and plutonium in the deep Sargasso Sea, *Deep-Sea Res., 32*, 273-286, 1985

Bauerfeind E., C. Garrity, M. Krumbholz, R.O. Ramseier and M. Voss, Seasonal variability of sediment trap collections in the Northeast Water Polynia. Part 2. Biochemical and microscopic composition of sedimenting matter, *J. Mar. Syst. 10*, 371-389, 1997

Behrenfeld, M.J., and P.G. Falkowski, Photosynthetic rates derived from satellite-based chlorophyll concentration, *Limnol. Oceanogr., 42*, 1-20, 1997

Berger, W.H., and G. Wefer, Export production: Seasonality and intermittency, and paleoceanographic implications, *Paloegeogr.,-Paleoclimatol.,-Paleoecol., 89*, 245-254, 1990

Berger, W.H., K. Fischer, C. Lai, and G. Wu, Ocean carbon flux: global maps of primary production and export production. In: *Biogeochemical cycling and fluxes between the deep euphotic zone and other oceanic realms*. C Agegian, editor, NOAA Undersea Res.Progr., 3, 1-44, 1987

Betzer, P.R., W.J Showers, E.A Laws, C.D Winn, G.R DiTullio, and P.M. Kroopnick, Primary productivity and particle fluxes on a transect of the equator at 153° W in the Pacific Ocean, *Deep-Sea Res., 31*, 1-11, 1984

Bodungen, B. von, A. N. Antia, E. Bauerfeind, O. Haupt, I. Peeken, R. Peinert, S. Reitmeier, C. Thomsen, M. Voss, M. Wunsch, U. Zeller, and B. Zeitzschel, Pelagic processes and vertical flux of particles: an overview over a long-term comparative study in the Norwegian Sea and Greenland Sea, *Geologische Rundschau 84*, 11-27, 1995

Bory, A.J.-M. and P.P. Newton, Transport of airborn lithogenic material sown through the water column in two contrasting regions of the eastern subtropical North Atlantic Ocean, *Global Biogeochemical Cycles, 14*, 297-315, 2000

Boyd, P.W., and P.P. Newton, Does planktonic community structure determine downward particulate organic carbon flux in different oceanic provinces? *Deep-Sea Res., 46*, 63-91, 1999

Buesseler, K.O., D.K. Steinberg, A.F. Michaels, R.J. Johnson, J.E. Andrews, J.R. Valdes, and J.F. Price, A comparison of the quantity and composition of material caught in a neutrally buoyant versus surface-tethered sediment trap, *Deep-Sea Res., 47*, 277-294, 2000

Buesseler, K.O., Do upper-ocean sediment traps provide an accurate record of the particle flux? *Nature, 353*, 420-423, 1991

Campbell, J.W, and T. Aarup, New production in the North Atlantic derived from seasonal patterns of surface chlorophyll, *Deep-Sea Res., 39*, 1669-1694, 1992

Conte, M. H., N. Ralph and E.H. Ross, Seasonal and interannual variability in deep ocean particle fluxes at the Ocean Flux Program (OFP) (Bermuda Atlantic Time Series (BATS) site in the western Sargasso Sea near Bermuda, *Deep-Sea Res., 48*, 1471-1505

Deuser, W.G., F.E. Muller-Karger, R.H. Evans, O.B. Brown, W.E. Esaias and G.C. Feldman, Surface ocean color and deep-ocean carbon flux: how close a connection? *Deep-Sea Res., 37*, 1331-1343, 1990

Deuser, W.G., Seasonal and interannual variations in deep-water particle fluxes in the Sargasso Sea and their relation to surface hydrography, *Deep-Sea Res., 33*, 225-246, 1986

Deuser, W.G., T.D. Jickells, P. King, and J.A. Commeau, Decadal and annual changes in biogenic opal and carbonate fluxes to the deep Sargasso Sea. *Deep-Sea Res., 42*, 1923-1995, 1995

Deuser, W.G., Temporal variability of Particle Flux in the Deep Sargasso Sea, *In: Particle Flux in the Ocean*, V.Ittekot, P. Schäfer, S. Honjo and P.J. Depetris, eds, Wiley, 1996

Dugdale, R.C., and J.J. Goering, Uptake of new and regenerated forms of nitrogen in primary productivity, *Limnol. Oceanogr., 12*, 196-206, 1967

Dugdale, R.C., F.P. Wilkerson, R.T. Barber and F.P. Chavez, Estimating New Production in the Equatorial Pacific Ocean at 150°W, *J. Geophys. Res., 97*, 681-686, 1992

Eppley, R.W. and B.J. Peterson, Particulate organic matter flux and planktonic new production in the deep ocean, *Nature, 282*, 677-680, 1979

Eppley, R.W., E.H. Renger and P.R. Betzer, The residence time of particulate oganic carbon in the

surface layer of the ocean, *Deep-Sea Res., 30*, 311-323, 1983

Falkowski, P.G., R.T. Barber, and V. Smetacek, Biogeochemical controls and feedbacks on ocean primary production, *Science, 281*, 200-206, 1998

Fischer, G., V. Ratmeyer, and G. Wefer, Organic carbon fluxes in the Atlantic and the Southern Ocean: relationship to primary production compiled from satellite radiometer data, *Deep-Sea Res., 47*, 1961-1997, 2000

Frankignoulle, M., C. Canon, and J.-P. Gattuso, Marine calcification as a source of carbon dioxide: Positive feedback of increasing atmospheric CO_2, *Limnol. Ogeanogr., 39*, 458-462, 1994

Gust, G., A.F. Michaels, R. Johnson, W.G.Deuser and W. Bowles, Mooring line motions and sediment trap hydromechanics: in situ intercomparison of three common deployment designs. *Deep-Sea Res., 41*, 831-857, 1994

Hebbeln, D. and G. Wefer, Effects of ice coverage and ice-rafted material on sedimentation in the Fram Strait, *Nature, 350*, 409-411, 1991

Hebbeln, D., Flux of ice-rafted detritus from sea ice in the Fram Strait, *DeepSea Res.II*, 47, 1773-1790, 2000

Honjo, S. and S.J. Manganini, Annual biogenic particle fluxes to the interior of the North Atlantic Ocean studied at 34°N 21°W and 48°N 21°W. *Deep-Sea Res., 40*, 587-607, 1993

Honjo, S., S.J. Manganini and G. Wefer, Annual particle flux and a winter outburst of sedimentation in the northern Norwegian Sea, *Deep-Sea Res.*, 35, 1223-1234, 1988

Jackson, J.E., A user´s guide to principal components. Wiley, New York, 569 pp., 1991

Jahnke, R., The global ocean flux of particulate organic carbon: Areal distribution and magnitude, *Global Biogeochem.Cycles, 10*, 71-88, 1996

Jenkins, W.J., Nitrate flux into the euphotic zone near Bermuda, *Nature, 331*, 521-523, 1988

Kähler, P. and E. Bauerfeind, Organic partclies in sediment traps: substantial losses to the dissolved phase, *Limnol. Oceanogr., 46*, xx-xx

Kano, J., Relation between increase of coral and atmospheric Carbon Dioxide Concentration, *Sora, 65*, 1-7, 1990

Karl, D., R. Letelier, L. Tupas, J. Dore, J. Christian and D. Hebel, The role of nitrogen fixation in biogeochemical cycling in the subtropical North Pacific Ocean, *Nature, 388*, 533-538, 1997

Kuss, J. and K. Kremling, Particulate trace elemental fluxes in the deep north-east Atlantic Ocean, *Deep-Sea Res., 46*, 149-169, 1999

Lampitt, R., Evidence for the seasonal deposition of detritus to the deep-sea floor and its subsequent resuspension, *Deep-Sea Res.*, 32, 885-897, 1985

Lampitt, R.S. and A.N. Antia, Particle flux in deep seas: regional characteristics and temporal variability, *Deep-Sea Res., 44*, 1377-1403, 1997

Lande, R. and A.M. Wood, Suspension times of particles in the upper ocean, *Deep-Sea Res., 34*, 61-72, 1987

Lohrenz, S.E., G.A. Knauer, V.L. Asper, M. Tuel, A.F. Michaels and A.H. Knap, Seasonal variability in primary production and particle flux in the northwestern Sargasso Sea: U.S. JGOFS Bermuda Atlantic Time-series Study, *Deep-Sea Res., 39*, 1373-1391, 1992

Longhurst, A., Ecological Geography of the Sea, Academic Press, London, pp 398

Longhurst, A., S. Sathyedranath, T. Platt and C. Caverhill, An estimate of global primary production in the ocean from satellite radiometer data, *J. Plankt. Res., 17*, 1245-1271, 1995

Michaels, A.F. and A.H. Knap, Overview of the U.S. JGOFS Bermuda Atlantic Time-series Study and the Hydrostation S program, *Deep-Sea Res., 43*, 157-198, 1996

Michaels, A.F., A.H. Knap, R.L. Dow, K. Gundersen, R.J. Johnson, J. Sorensen, A. Close, G.A. Knauer, S.E. Lohrenz and V.A. Asper, Seasonal patterns of ocean biogeochemistry at the U.S. JGOFS Bermuda Atlantic Time-series Study Site, *Deep-Sea Res., 41*, 1013-1038, 1994

Milliman, J.D., P.J. Troy, W.M. Balch, A.K. Adams, Y.H. Li and F.T. Mackenzie, Biologically mediated dissolution of calcium carbonate above the chemical lysocline? *Deep-Sea Res., 46*, 1653-1669, 1999

Monterey, G. and S. Levitus, Seasonal Variability of Mixed Layer Depth for the World Ocean. *NOAA Atlas NESDIS 14*, U.S. Gov. Printing Office, Wash., D.C., 96 pp., 1997

Mortlock, R.D. and P.N. Fröhlich, A simple method for the rapid determination of biogenic opal in pelagic marine sediments, *Deep-Sea Res., 36*, 1415-1426, 1989

Najjar, R.G. and R.F. Keeling, Mean annual air-sea oxygen flux: A global view, *Global Biogeochem. Cycles, 14*, 573-584, 2000

Neuer, S., V. ratmeyer, R. Davenport, G. Fischer and G. Wefer, Deep water particle flux in the Canary Island region: seasonal trends in relation to long-term satellite derived pigment data and lateral sources, *Deep-Sea Res., 44*, 1451-1466, 1997

Newton, P.P., R.S. Lampitt, T.D. Jickells, P. King and C. Boutle, Temporal and spatial variability of biogenic particle fluxes during the JGOFS northeast

Atlantic process studies at 47°N 20°W, *Deep-Sea Res., 41*, 1617-1642

Noji, T.T., K.Y. Borsheim, F. Rey and R. Norvedt, Dissolved organic carbon associated with sinking particles can be crucial for estimates of vertical carbon flux, *Sarsia, 84*, 129-135, 1999

Oschlies, A. and V. Garcon, Eddy-induced enhancement of primary production in a model of the North Atlantic Ocean, *Nature, 394*, 266-269, 1998

Pace, M.L., G.A. Knauer, D.M. Karl and J.H. Martin, Primary production, new production and vertical flux in the Eastern Pacific, *Nature, 325*, 803-804, 1987

Peinert, R., A. N. Antia, E. Bauerfeind, O. Haupt, M. Krumbholz, I. Peeken, B.v. Bodungen, R. Ramseier, M. Voss and B. Zeitzschel, Particle flux variability in the Polar and Atlantic biogeochemical provinces of the Nordic Seas. In,*The Northern North Atlantic: a changing environment*, P. Schäfer, W. Ritzrau. M. Schlüter and J. Thiede, eds. Springer, Berlin, pp 53 – 68, 2001

Rey, F., Development of the spring phytoplankton outburst at selected sites off the Norwegian coast, in *The Norwegian Coastal Current*, R. Saetre and M. Mork, eds., *2*, 649-680, 1991

Riebesell, U., I. Zondervan, B. Rost, P.D. Tortell, R. E. Zeebe and F.Morel, Reduced calcification of marine plankton in response to increased atmospheric CO_2, *Nature, 407*, 364–367, 2000

Sarnthein, M., U. Pflaumann, R. Ross, R. Tiedemann and K. Winn, Transfer functions to reconstruct ocean paleoproductivity: a comparison, *In: Upwelling Systems: Evolution since the early Miocene*, Summerhayes, C.P., W.L. Prell and K.C. Emeis, eds, Geological Society Special Publication, *64*, 411-427, 1992

Schlitzer, R., Applying the adjoint Method for Biogeochemical Modelling in *Inverse Methods in Global Biogeochemical Cycles*, P. Kasibhatla, M. Heimann, D. Hartley, N. Mahowald, R. Prinn and P. Rayner, eds., pp 107-124, , AGU Geophys. Monograph Series, 1999.

Schlüter, M., E.J. Sauter, A. Schäfer and W. Ritzrau, Spatial budget of organic carbon flux to the seafloor of the northern North Atlantic (60°N – 80°N), *Global Biogeochem. Cycles, 14*, 329-340

Scholten, J. C., F. Fietzke, S. Vogler, M. Rutgers van der Loeff, A.Mangini, W. Koeve, J. Waniek P. Stoffers, A. Antia and J. Kuss, Trapping efficiency of sediment traps from the deep eastern North Atlantic: ^{230}Th calibration, *Deep-Sea Res. II, 48*, 243-268.

Siegel, D.A. and W.G. Deuser, Trajectories of sinking particles in the Sargasso Sea: modelling of "statistical funnels" above deep-ocean sediment traps, *Deep-Sea Res., 44*, 1519-1541, 1997

Smith, S.V. and F.T. Mackenzie, Comments on the role of oceanic biota as a sink for anthropogenic CO_2, *Global Biogeochem. Cycles, 5*, 189-190, 1991

Steinberg, D.K., C.A. Carlson, N.R. Bates, R.J. Johnson, A.F. Michaels and A.H. Knap, Overview of the US JGOFS Bermuda Atlantic Time-series Study (BATS): a decade look at ocean biology and biogeochemistry, *Deep-Sea Res., 48*, 1405-1447, 2001

Suess, E., Particulate organic carbon flux in the oceans-surface productivity and oxygen utilisation, *Nature, 288*, 260-263, 1980

Tsunogai, S. and S. Noriki, Particulate fluxes of carbonate and organic carbon in the ocean. Is the marine biological activity working as a sink of the atmospheric carbon? *Tellus, 43*, 256-266, 1991

Waniek, J., W. Koeve and R.S. Prien, Trajectories of sinking particles and the catchment areas in the North East Atlantic, *J. Mar. Res., 58*, 983-1006, 2000

Wassmann, P., Retention versus export food chains: processes controlling sinking loss from marine pelagic systems, *Hydrobiologia, 363*, 29-57, 1998

Wefer, G. and G. Fischer, Annual primary production and export flux in the Southern Ocean from sediment trap data, *Marine Chemistry, 35*, 597-613, 1991

Wefer, G. and G. Fischer, Seasonal patterns of vertical particle flux in equatorial and coastal upwelling areas of the eastern Atlantic, *Deep-Sea Res., 40*, 1613-1645, 1993

Wefer, G., W.H. Berger, J. Bijma and G. Fischer, Clues to Ocean history: a brief Overview of Proxies, In: *Use of Proxies in Paeoceanography: Examples from the South Atlantic*, G. Fischer and G. Wefer, eds., Springer Verlag, Heidelberg, pp 1-68, 1999